

Adsorption of Phosphate on Nano-ball Allophane, Change
in Charge Characteristics Induced by the Adsorption, and
Mechanism Analysis by Molecular Orbital Method

(ナノボール状アロフェンにおけるリン酸吸着と吸着によって
引き起こされる荷電特性変化およびメカニズムの
分子軌道法解析)

Erni Johan

1999

①

DOCTORAL DISSERTATION

Adsorption of Phosphate on Nano-ball Allophane, Change
in Charge Characteristics Induced by the Adsorption, and
Mechanism Analysis by Molecular Orbital Method

ナノボール状アロフェンにおけるリン酸吸着と吸着によって
引き起こされる荷電特性変化およびメカニズムの
分子軌道法解析

by

Erni Johan

Submitted to

The United Graduate School of Agricultural Sciences

Ehime University, Japan

in Partial Fulfillment of the Requirements for
the Degree of Doctor of Agriculture

Department of Life Environment Conservation Science

United Graduate School of Agricultural Sciences

Ehime University, Japan

March, 1999

学位論文要旨

氏名 Erni Johan

論文名 Adsorption of Phosphate on Nano-ball Allophane, Change in Charge Characteristics Induced by the Adsorption, and Mechanism Analysis by Molecular Orbital Method

(ナノボール状アロフェンにおけるリン酸吸着と吸着によって引き起こされる荷電特性変化およびメカニズムの分子軌道法解析)

Summary

On the basis of recent information on the chemical structure of allophane with nano-ball morphology, study on phosphate adsorption was carried out on pure allophane samples ($<0.2 \mu\text{m}$), separated from inner part of weathered pumice grains, collected from different sites in Japan. The samples were different in Si/Al ratio, KyP with Si/Al=1.34:2 and KnP with Si/Al=1.98:2. The sample KnP with high Si/Al ratio contains much more weakly bonded SiO_4 tetrahedra on its structure, than the sample KyP with the low ratio. The objectives of this study were to analyze mechanism of phosphate adsorption in detail, and to know changes in surface characteristics of the allophane, due to the adsorption. Theoretical molecular orbital calculation was applied to elucidate the detailed mechanism in the atomic and electron levels.

Phosphate adsorption was done at low phosphate concentration, up to 2 mM of H_2PO_4^- in order to avoid dissolution or disruption of allophane. The adsorption was done in the solutions containing sodium and calcium ions as background. Parts of allophane-phosphate adsorption complexes (samples with P adsorbed on them) were subjected for measurements in surface acidity, cation exchange capacity (CEC), and anion exchange capacity (AEC). For molecular orbital calculation, MOPAC program was used with semi-empirical MNDO-PM3 basis set which is incorporated in CHAChe system for Windows.

The results indicated that KyP was greater in the phosphate adsorption

than the KnP, that was ascribed to much more content of aluminol groups (Al-OH, Al-OH₂) per unit mass for the KyP. The silicon release was observed within all ranges of P adsorption, and plotting the Si release against P adsorption resulted in linear relationship. The KnP sample released much more silicon than the KyP samples. Based on above finding, new adsorption mechanism was proposed, namely replacement of polymeric SiO₄ tetrahedra with phosphate, as shown below:



Possibility of the reaction was proven by negative value of the change in heats of formation, ΔH , obtained by molecular orbital calculation.

Acid strength increased after the P adsorption for both KyP and KnP samples. The increase in the acidity was observed for both sodium and hydrogen saturated samples. For the hydrogen saturated, only Brønsted acid existed, leading to conclusion that the Brønsted acidity increased due to the P adsorption. Calculation by molecular orbital method proved that the increase in the acidity is not due to P-OH groups newly formed on the adsorption complexes but due to strengthening in Brønsted acidity of silanol groups (Si-OH) originally present in the structure of allophane. Interaction between P-OH and Si-OH may occur in electron level to accelerate the dissociation of proton from the silanol groups. The study suggested that some of acid sites of allophane and allophane-phosphate adsorption complex also acted as negative charge for cation exchange capacity sites.

Observed changes in the amounts of negative and positive charges of allophane with phosphate adsorption (NaH₂PO₄ in NaCl with total [Na]=10 mM) were interpreted in terms of two reasons. One reason is base on increase in solution pH, variable charge characteristics, and the other is on net effect caused by the adsorbed phosphate. The net effect increased negative charge and decreased positive charge of allophane. To explain the net effect, it is assumed that OH⁻ was initially released in just the same amount as the adsorbed H₂PO₄⁻ from allophane-phosphate adsorption complex. This situation is comparable with that when the same equivalent amount of NaOH was added to original allophane. The comparison indicated that the Si-OH and Al-OH₂⁺ functional groups of the adsorption complex had higher ability to react with the OH⁻ than those of the original allophane. An inductive effect of the adsorbed phosphate, which accelerated deprotonation reaction of inherent functional groups such as Si-OH and Al-OH₂⁺ of allophane, was suggested by theoretical molecular orbital calculations.

Key words: Nano-ball allophane, Phosphate adsorption, Surface acidity, Charge characteristics, Molecular orbital method

ACKNOWLEDGMENTS

I am pleased in expressing my heart felt thanks and deep sense of gratitude to my supervisor, Prof. Teruo Henmi, for his advise, laudable counseling and guidance through out the period of this research. I would like to acknowledge very sincerely to Dr. Naoto Matsue, for his valuable suggestions and patiently guidance during the research and preparing the dissertation. They provided continuos encouragement on my study. I am really indebted and proud to them.

My thank also go to Prof. Katsutoshi Sakurai, Professor from Department of Bio-resource, Kochi University for his helpful criticisms on my study. I thank to Prof. Yuuji Sakurai from Ehime University and to Dr. Tomoyuki Ishida, associate Professor from Kagawa University.

I would like to express my sincere gratitude to the Japanese Government, Ministry of Education, Science and Culture (Monbusho) for giving me the opportunity of studying in Japan, and providing me financial support through its international fellowship program. Appreciation is expressed to the Consul General of the Republic of Indonesia and the staffs in Osaka for their help in providing my personal

documents.

I thank my friends Mr. Le Thanh Son and Mr Ryohei Ochi, who help me so much. We used to discuss our researches and talk many interesting topics. I got much knowledge about Vietnam and Japan from them. My thanks also go to the students in Soil Science laboratory for their friendship and hearty cooperation.

Most of all, I would like to express my love and appreciation to my husband. Without his patient and understanding I can not accomplish this work. Finally I would like to give my hearty thanks to my mother and my father, for their support and assistance during my study.

List of Contents

	Page
ACKNOWLEDGMENTS	i
List of Contents	iii
List of Figures	vi
List of Tables	x
Chapter 1 INTRODUCTION	1
1-1 Phosphorus in Environment	1
1-2 Phosphorus in Agriculture	3
1-3 Allophane	4
Chapter 2 MINERALOGICAL CHARACTERISTICS OF ALLOPHANE	10
2-1 Sample Preparations	10
2-2 Identification of Clay Samples	12
2-2-1 X-ray Powder Diffraction Pattern	12
2-2-2 Infrared Spectroscopy	14
2-2-3 Differential Thermal Analysis	18
2-3 Conclusions	20

Chapter 3 PHOSPHATE ADSORPTION ON ALLOPHANE AND ITS MECHANISM BY MEANS OF MOLECULAR ORBITAL METHOD	21
3-1 Introduction	21
3-2 Materials and Methods	23
3-3 Results and Discussion	25
3-3-1 Phosphate Adsorption Isotherm	25
3-3-2 Langmuir Adsorption Equation	29
3-3-3 Silicon Release	34
3-3-4 Molecular Orbital Analysis	37
3-3-5 Change in Allophane Structure after the P Adsorption	42
3-3-5-1 Differential Thermal Analysis	42
3-3-5-2 Infrared Spectroscopy	45
3-4 Conclusions	51
Chapter 4 CHANGE IN SURFACE ACIDITY OF ALLOPHANE WITH P ADSORPTION	53
4-1 Introduction	53
4-2 Materials and Methods	58
4-3 Results and Discussion	62
4-3-1 Samples with Sodium Saturation	62
4-3-2 Samples with H Saturation	71
4-3-3 Analysis by Molecular Orbital Method	75
4-4 Conclusions	83

Chapter 5 CHANGE IN THE SURFACE CHARGE WITH P ADSORPTION ON ALLOPHANE	84
5-1 Introduction	84
5-2 Materials and Methods	87
5-3 Results and Discussion	89
5-3-1 Net Effect of Phosphate Adsorption on charges	89
5-3-2 New Proposal for Adsorption Scheme	98
5-3-3 Molecular Orbital Analysis	110
5-4 Conclusions	114
 Chapter VI IMPLICATIONS OF THIS STUDY FOR AGRICULTURE AND ENVIRONMENT	 115
 REFERENCES	 117
 APPENDIX	 127

List of Figures

	Page
Fig. 1 Scheme of chemical structure of a unit particle of nano-ball shaped allophane (A: molecular morphology in section; B: atomic arrangement near the hole of hollow particle; C: atomic arrangement in the cross section of allophane particles)	7
Fig. 2 X-ray diffraction patterns of the allophane samples	13
Fig. 3 Infrared spectra of the allophane samples	15
Fig. 4 DTA curves of the allophane samples	19
Fig. 5 Phosphate adsorption isotherm of the Allophane samples	26
Fig. 6 Langmuir isotherm for adsorption of phosphate by the samples. C: equilibrium P concentration (mmol L^{-1}), X: amount of P adsorbed (mmol kg^{-1})	30
Fig. 7 Relationship between amount of P adsorbed and the amount of Si and Al released of the allophane samples	35
Fig. 8 Model clusters of allophane used for molecular orbital calculation	39

Fig. 9 DTA curves of the KyP sample before and after the P adsorption (amounts of P adsorbed are expressed in mmol kg ⁻¹)	43
Fig. 10 DTA curves of the KnP sample before and after the P adsorption (amounts of P adsorbed are expressed in mmol kg ⁻¹)	44
Fig. 11 Infrared spectra of KyP at various amounts of P adsorbed (the figure expressed amounts of P adsorbed in mmol kg ⁻¹)	46
Fig. 12 Infrared spectra of KnP at various amounts of P adsorbed (the figure expressed amounts of P adsorbed in mmol kg ⁻¹)	47
Fig. 13 Differential infrared spectra of phosphate adsorbed on KyP at various amounts of P adsorbed (a=845; B=869; c=617; d=609; e=296 mmol kg ⁻¹)	49
Fig. 14 Differential infrared spectra of phosphate adsorbed on KnP at various amounts of P adsorbed (a=651; B=594; c=532; d=457 mmol kg ⁻¹)	50
Fig. 15 Infrared spectra of the allophane samples before and after heating treatment at 105°C	70

Fig. 16 Cluster models of allophane used for molecular orbital calculation for the surface acidity	78
Fig. 17 Scheme of interaction between Si-OH and P-OH	82
Fig. 18a Charge characteristics of KyP samples in 10mM NaCl, with 0 and 25 cmol kg ⁻¹ P adsorption	90
Fig. 18b Charge characteristics of KnP samples in 10mM NaCl, with 0 and 20 cmol kg ⁻¹ P adsorption	91
Fig. 19 Schematic relationships among observed change, change due to pH effect and net change in surface negative and positive charges	95
Fig. 20 Summary of pH vs. negative charge curves of KyP and KnP samples with and without phosphate adsorption. KiG: imogolite sample with Si/Al=1:2	97
Fig. 21 Schematic representations for initial stage of reactions with OH ⁻ . A: allophane + NaOH; b: phosphated allophane + initially released OH ⁻	105

Fig. 22 Calculated H (heat of formation) of some molecules. I: phosphate bonded on two aluminol groups, II: phosphate replaced with silicon

List of Tables

	page
Table 1 Adsorption maxima (X_m) and binding energy constants (K) of the allophane samples	33
Table 2 Calculated ΔH (change in heat of formation) for equations (2), (3) and (4)	41
Table 3 List of Hammett indicators used for the surface acidity measurement	60
Table 4 Ordinary numbers to express H_0 values	61
Table 5 Measured acid strength (H_0) of the samples Before and after the P adsorption (Na-type)	63
Table 6a Possible origin of surface acidity of allophane before P adsorption	68
Table 6b Possible origin of surface acidity of allophane after the P adsorption	69
Table 7 Measured acid strength of the allophane samples after P adsorption followed by H^+ saturation	72
Table 8 Calculated heat of formation (H) of some dissociated and undissociated molecules	79
Table 9 Equilibrium solution pH after P adsorption ($K_{yP}=25 \text{ cmol kg}^{-1}$, $K_{nP}=20 \text{ cmol kg}^{-1}$) and after adding NaOH in same amount with P adsorbed	109

Chapter 1 INTRODUCTION

1-1. Phosphorus in Environment

Recently, an issue has arisen correlating to degradation of quality of life environment. Many researches have conducted some works in relation to environmental protection. One of the problems came from industrial and domestic waste water (WW) which were drained to rivers, lakes, or swamps.

Drainage of WW into waterways can frequently accelerate eutrophication on lakes, swamps, and reservoirs. Phosphorus (P) has been identified as the nutrient most likely limiting primary productivity in lakes and streams (Enfield and Ellis, 1986). Phosphorus typically constitutes less than 1% of total dissolved solids in municipal WW (Hook, 1986). The P contamination is great problem in water area such as lakes and streams. Surface water is often contaminated with P from wastes in intensive animal farming areas. For example, effluent from poultry manure contained 5 ppm P (161 μM) and a stream beside an intensive cow unit 2.6 ppm P (84 μM) when the waters were sampled

in East Suffolk in spring 1969 (Cooke and Williams, 1973).

The above problems have induced the impetus for application of the WW to land. That application, it was presumed, would utilize the soils well known P adsorption capacity to prevent WW from entering surface water (Hook, 1986). Effectiveness of soil is depend on its texture, permeability, kind of clay minerals, and the most important is capacity of soil to adsorb P. Therefore, study of P adsorption on soil materials is important not only for agriculture, but also in view of the environmental science.

When phosphorus (either as fertilizer or wastewater) are added to soil with low P adsorption capacity and high permeability, some parts of soluble P will be transported through percolate water and accumulated to groundwater. This will cause groundwater contamination. In that case soil plays an important role as a "filter" to protect the contamination, particularly for soils with medium or high P adsorption capacity.

1-2 Phosphorus in Agriculture

In view of agriculture, study of P adsorption on soil materials is necessary mainly to predict the P requirements and availability for plant growing in the relevant soil. Woodruff and Kamprath (1965) found that soils with low P adsorption capacity required higher P concentration for maximum growth of plants. Thus, the previous P treatment often helped soil solution to maintain high P concentration for a longer period of time.

The P adsorption phenomenon often determines the fate and behavior of phosphorus in soil environment. The ability of a soil to adsorb or fix phosphorus is dependent on the texture, structure, and the most important factor is clay mineral composition. Soils containing ferric and aluminum oxide or hydroxide or allophanic clays are known to have high capacity for P retention (Parfitt, 1977). This phenomenon can cause severe deficiencies on P in plant due to phosphate fertilizer applied to them become not available for plants. However, after passing several years, the retained phosphorus will be released to soil solution

and became available for plants.

Previous studies on P adsorption however, were mainly focused on interactions with soil as such under the condition with relatively high P concentrations. The mechanism of P adsorption in soil environment is not so clear due to the presence of various components in the environment, such as organic matters, clay minerals, and ferric or aluminum oxides and hydroxides. Study of P adsorption on a single clay mineral is important to elucidate mechanism in detail. On the basis of chemical structure of allophane that is found recently, now became possible to discuss the mechanism in detail.

1-3 Allophane

Several decades ago, allophane was only recognized as an amorphous materials (without form), which was usually found in soils developed from volcanic ash or pumice, such as Andepts. However, recent investigations using electron microscopy, X-ray diffraction, infrared (IR) spectroscopy, differential thermal analysis (DTA), and nuclear

magnetic resonance (NMR), has established the morphology and chemical structure of allophane (Henmi, 1980; Henmi and Wada, 1976; Shimizu et al., 1988).

Allophane is defined as naturally occurring amorphous hydrous aluminosilicates of various chemical composition, which are characterized by the predominance of Si-O-Al bondings (van Olphen, 1971). Fundamental structure of Allophane is composed of gibbsite $[Al(OH)_3]$ sheet with SiO_4 tetrahedra attaching on it, and has hollow spherical morphology to locate the SiO_4 tetrahedra inside of the sphere (Parfitt and Henmi, 1980). Wall of the hollow sphere, nano-ball, has some holes (defects) with diameter of 0.3-0.5 nm, resulting in Al-OH and Al-OH₂ groups exposed (Paterson, 1977; Wada and Wada, 1977). Since the allophane has hollow sphere or ball shape and nano level in size (3.5-5.0 nm), that relatively smaller than other clay minerals, here **nano-ball (shaped) allophane** is used as a new term for allophane. Furthermore, the term allophane always refers to nano-ball shaped allophane.

Allophane has a narrow range of chemical

composition from 1:2 to 2:2 with respect to Si/Al atomic ratio (Henmi and Wada, 1976). Fundamental structure of allophane is that with Si/Al ratio of 1:2 (Henmi, 1985). The structure contains all of the SiO_4 tetrahedra in the monomeric form (orthosilicate type), with walls of the spherules built up largely from imogolite structure units $[(\text{OH})_2\text{Al}_2\text{O}_3\text{SiOH}]$ with some defects or pores, and often called proto-imogolite allophane (Parfitt and Henmi, 1980; Farmer et al., 1980). That type of allophane is quite rarely found in nature. Allophane with the Si/Al ratio more than 1:2 has some condensed SiO_4 tetrahedra weakly bonded to its structure (Parfitt et al., 1980). The condensed SiO_4 tetrahedra is also called accessory materials, so that allophane with higher Si/Al ratio contains much more the accessories. Schematic chemical structure of nano-ball shaped allophane is given in Fig. 1. The figure shows some pores or defect part on allophane structure that were produced by omitting two Si and two Al atoms from six imogolite unit cells. The pores exhibit aluminol groups (Al-OH or Al-OH₂), whereas inside part of allophane shows silanol groups (Si-OH). The two functional groups

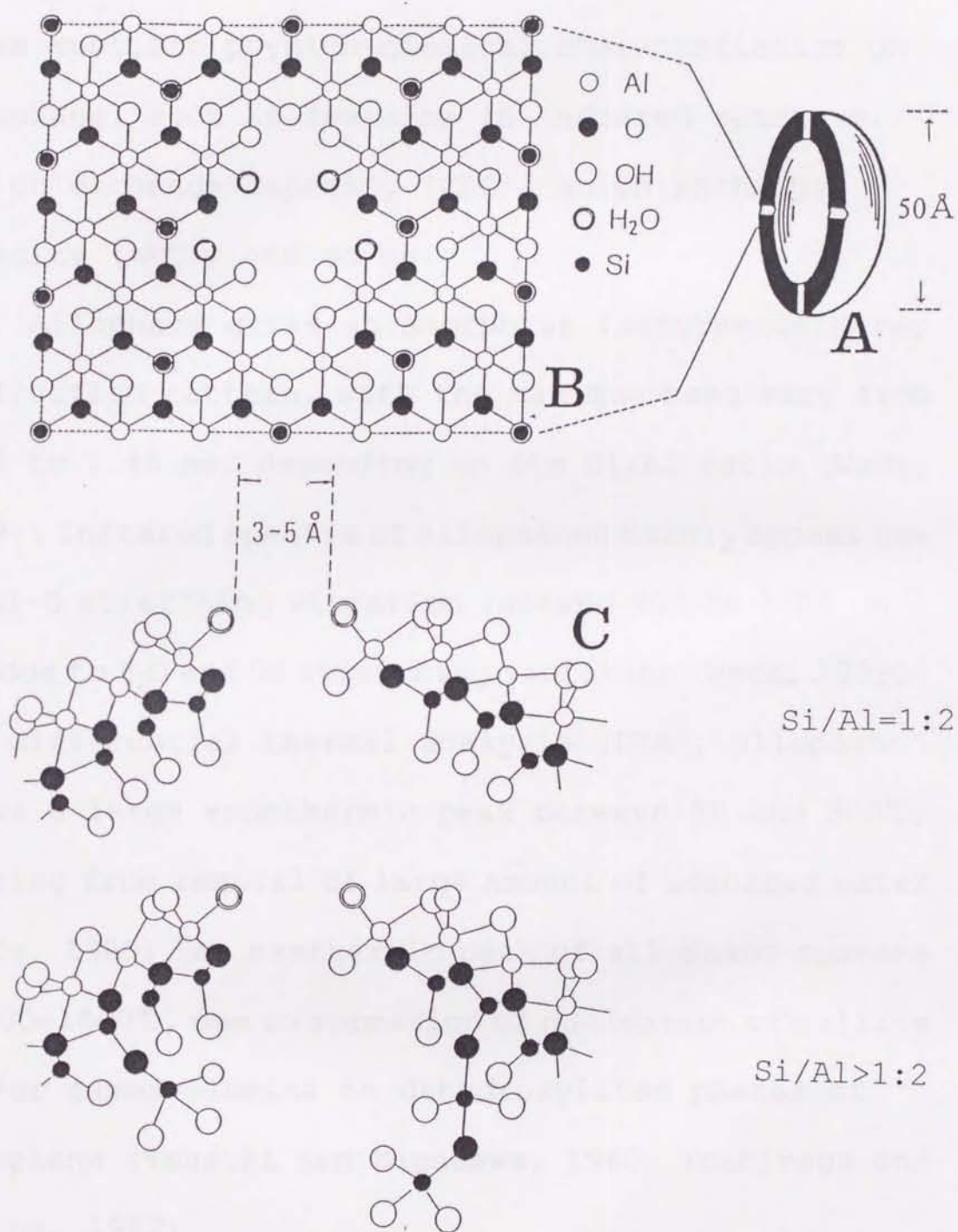


Fig. 1 Scheme of chemical structure of a unit particle of nano-ball shaped allophane (A: molecular morphology in section; B: atomic arrangement near the hole of hollow particle; C: atomic arrangement in the cross section of allophane particles)

cause specific physico-chemical characteristics on allophane, such as features in infrared spectrum, cation exchange capacity (CEC), anion exchange capacity (AEC), and so on.

Allophane gives an amorphous features in X-ray diffraction pattern, with the maximum band vary from 1.23 to 1.45 nm, depending on its Si/Al ratio (Wada, 1989). Infrared spectra of allophanes mainly appear due to Si-O stretching vibration (around 900 to 1000 cm^{-1}) and due to H₂O and OH stretching vibration (Wada, 1989). For differential thermal analysis (DTA), allophane shows a large endothermic peak between 50 and 300°C, arising from removal of large amount of adsorbed water (Wada, 1989). An exothermic peak of allophane appears at 900-1000°C, due to formation or nucleation of mullite and/or gamma alumina in dehydroxylated phases of allophane (Tsuzuki and Nagasawa, 1960; Yoshinaga and Aomine, 1962).

The objectives of this study were to understand the clear mechanism of phosphate adsorption on allophane, in relation to its chemical structure, and

to know change in physicochemical properties of allophane due to the adsorption. Molecular orbital analysis was carried out to simulate theoretically possible reactions, which is impossible to be examined through experiment in laboratories. Here, allophane was chosen as an adsorbent since it has high capacity for anion adsorption, and it is major component in Andepts.

Chapter 2 MINERALOGICAL CHARACTERISTICS OF

ALLOPHANE

2-1 Sample Preparations

Allophane samples were separated from inner part of weathered pumice grains, collected from two volcanic ash soils of Japan: Kurayoshi, Tottori prefecture and Kakino, Kumamoto prefecture, for KyP and KnP sample, respectively. Outer parts of pumice grains were removed, then inner parts were ground. The ground pumice were suspended in water, then were dispersed with ultrasonification at 28 kHz. Suspension pH was adjusted at 4 for allophane sample with low Si/Al ratio (KyP), or at pH 10 for that with high Si/Al ratio (KnP). The suspensions were placed in 1 L of cylinders, and were shaken reciprocally with hand, then were stand overnight to allow sedimentation for silt and sand particles. Then, clay fraction ($< 2 \mu\text{m}$) was separated by pipette method at 25 cm depth. The fraction was flocculated with NaCl then supernatant was discarded.

Fine clay fraction ($< 0.2 \mu\text{m}$) was separated from the clay fraction by centrifugation at pH 4 for sample

having low Si/Al ratio (KyP), or at pH 10 for that with high Si/Al ratio (KnP). Collected fine clay fraction was flocculated with saturated NaCl, then were washed with water to remove excess NaCl. The samples were subjected for X-ray diffraction, for infrared (IR) spectrophotometry, and for differential thermal analysis (DTA) to examine their purity. The samples were stored as suspensions. Those suspensions were used for the whole experiments. Such manner of separation (<0.2 μ m fractions) avoids possible contamination of impurities such as volcanic glasses, opaline silica, and imogolite (Henmi and Wada, 1976).

Dissolution of allophane samples was carried out with 0.15 M sodium oxalate solution of pH 3.5 according to the method of Higashi and Ikeda (1974). After dissolution, Si, Al and Fe were measured for the solutions by atomic absorption spectrophotometry (AAS). The results indicated that the samples contain 39.41 and 37.02% of SiO₂ and Al₂O₃, respectively for KyP, and 40.24 and 34.45% for KnP. The Si/Al ratios were calculated as 1.34:2 and 1.98:2, for KyP and KnP, respectively. The Si/Al ratio of natural and synthetic

allophane samples usually range from 1:2 to 2:2 (Henmi and Wada, 1976; Parfitt and Henmi, 1980; Wada, 1989; Henmi et al., 1981), so the KnP sample belongs to allophane with high Si/Al ratio, and has more accessory, polymeric SiO₄ tetrahedra in its structure (Shimizu et al., 1988; Henmi et al., 1997).

2-2 Identification of Clay Samples

2-2-1 X-ray Powder Diffraction Pattern

Figure 2 shows the X-ray diffraction pattern, for the KyP and KnP samples. The allophane samples show three broad diffraction bands with maxima at 0.345, 0.225 and 0.142-0.145 nm with intensities of strong, medium, and weak. There is almost no deference in the bands between KyP and KnP samples. That bands were similar with former investigations (Yoshinaga and Aomine, 1962; Henmi et al., 1981). Farmer et al. (1977) suggested that the latter two bands corresponded in position to 63 (0.225 nm) and 06 (0.140 nm) reflections of imogolite and might be ascribed to the "imogolite structure". In fact, allophane and imogolite have same basic structure, namely gibbsite with one

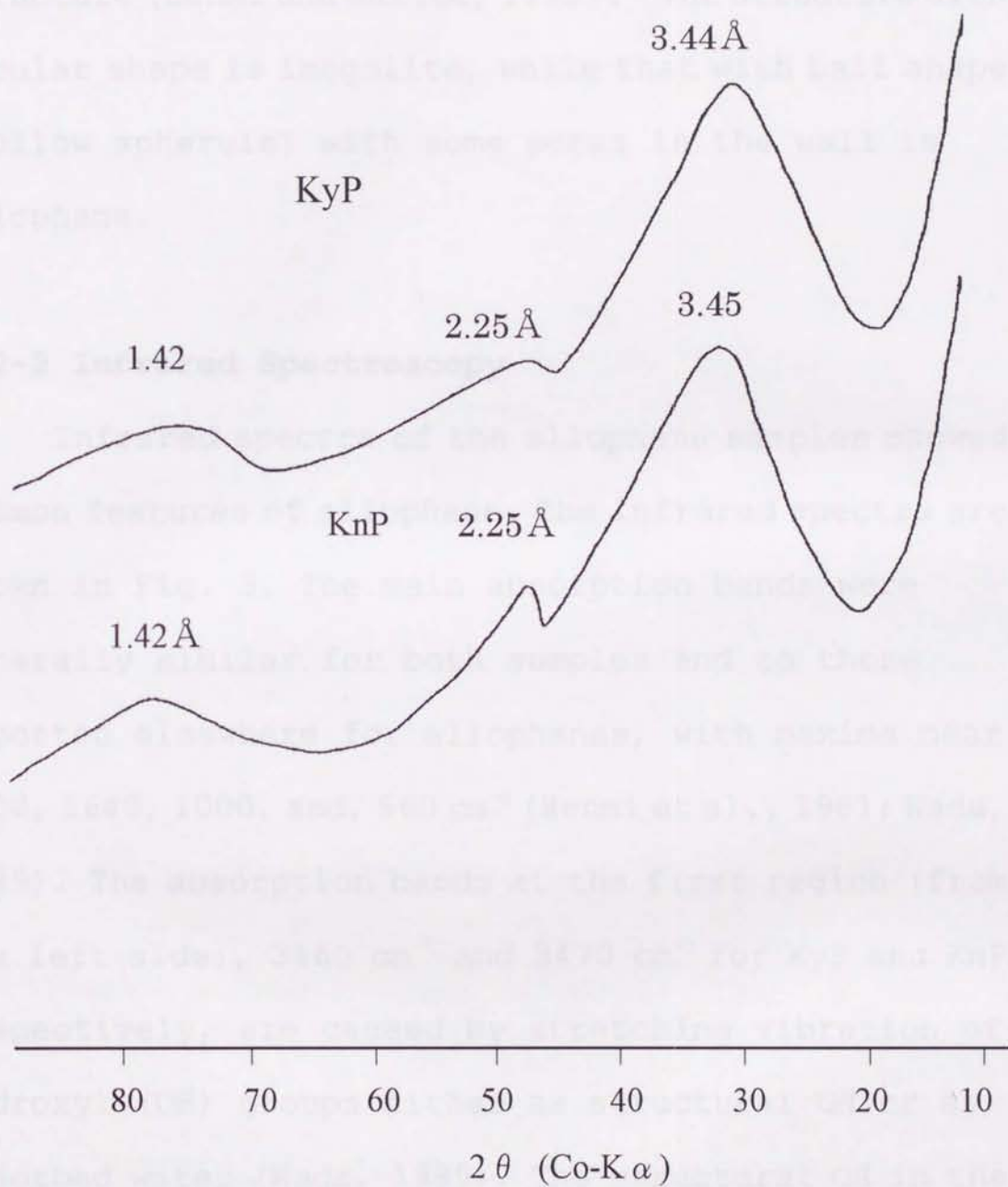


Fig. 2 X-ray diffraction patterns of the allophane samples

orthosilicate occupying the vacant site in its structure (Henmi and Matsue, 1998). The structure with tubular shape is imogolite, while that with ball shape (hollow spherule) with some pores in the wall is allophane.

2-2-2 Infrared Spectroscopy

Infrared spectra of the allophane samples showed common features of allophane. The infrared spectra are shown in Fig. 3. The main absorption bands were generally similar for both samples and to those reported elsewhere for allophanes, with maxima near 3400, 1640, 1000, and, 560 cm^{-1} (Henmi et al., 1981; Wada, 1989). The absorption bands at the first region (from the left side), 3460 cm^{-1} and 3470 cm^{-1} for KyP and KnP respectively, are caused by stretching vibration of hydroxyl (OH) groups either as structural OH or as adsorbed water (Wada, 1989). The structural OH in the structure of allophane present as Si-OH or Al-OH groups. Intensity of that band decreases with heating treatment at around 300°C, due to loss of adsorbed water and some hydroxyl groups (dehydration and dehydroxylation)

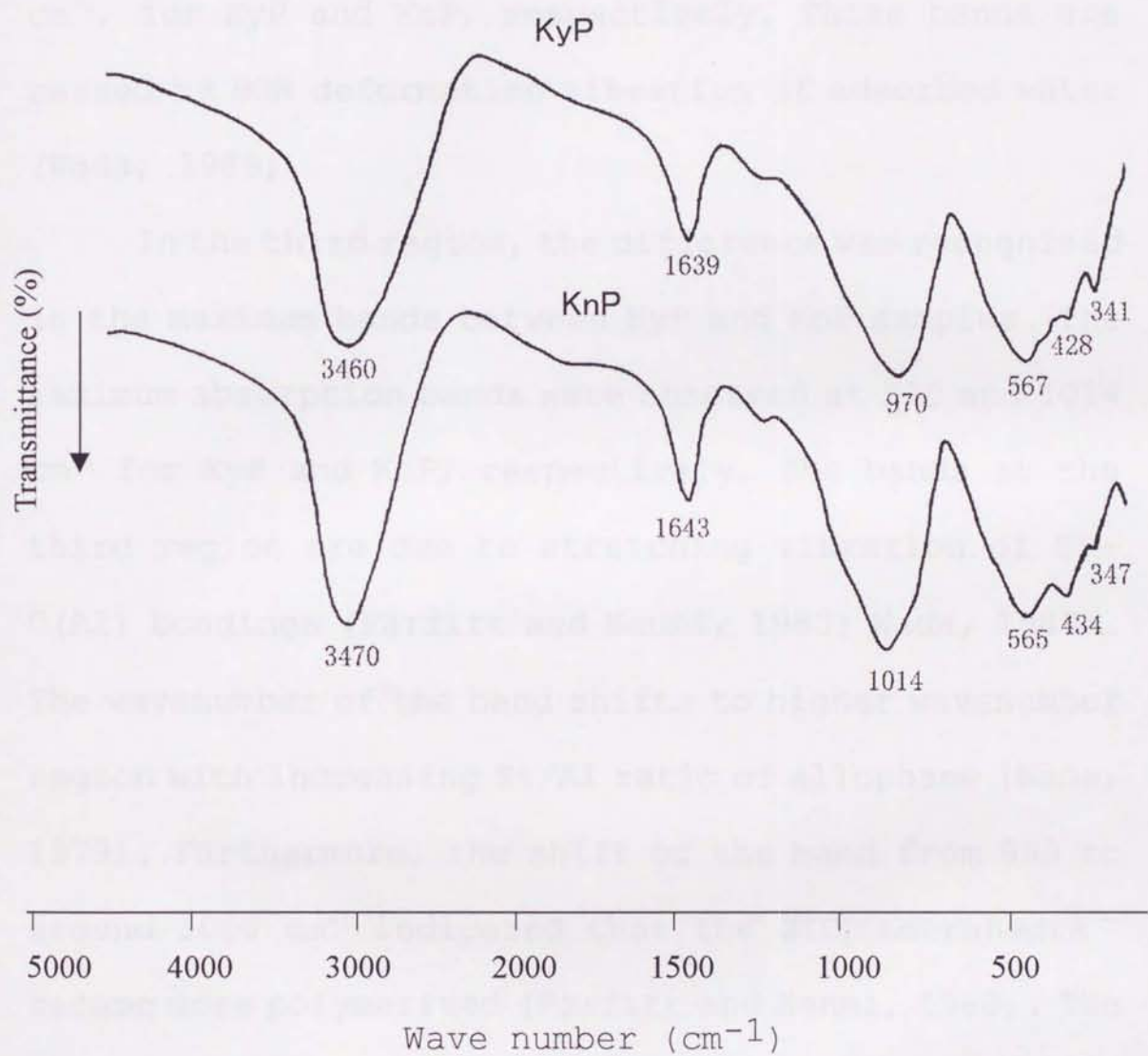


Fig. 3 Infrared spectra of the allophane samples

(Henmi and Wada, 1974). In the second region, the maximum adsorption bands were observed at 1639 and 1643 cm^{-1} , for KyP and KnP, respectively. Those bands are caused by HOH deformation vibration of adsorbed water (Wada, 1989).

In the third region, the difference was recognized in the maximum bands between KyP and KnP samples. The maximum absorption bands were observed at 970 and 1014 cm^{-1} for KyP and KnP, respectively. The bands at the third region are due to stretching vibration of Si-O(Al) bondings (Parfitt and Henmi, 1980; Wada, 1989). The wavenumber of the band shifts to higher wavenumber region with increasing Si/Al ratio of allophane (Wada, 1979). Furthermore, the shift of the band from 960 to around 1000 cm^{-1} indicated that the SiO_4 tetrahedra became more polymerized (Parfitt and Henmi, 1980). The present data showed that the absorption band of KnP is higher than that of KyP, indicating that KnP has higher Si/Al ratio than KyP has, as observed on the results of chemical analysis. This indicated that KnP contained much more polymerized SiO_4 .

The maximum absorption band in the fourth region

appears at 567 and 565 cm^{-1} for KyP and KnP, respectively. Those bands suggest that allophane samples contain common, unique Al-OH structure (Wada, 1989). That band was also observed for synthetic allophane and imogolite (Farmer et al., 1979; Wada et al., 1979; Parfitt et al., 1980), hydroxy-Al silicate cations, and even polymer hydroxy-Al ions (Farmer et al., 1979; Wada and Wada, 1980).

In addition to the four major bands, the IR spectra also exhibited two side bands near 430 and 340 cm^{-1} . The first side band could be attributed to condensation of the silica component because it occurred in parallel with that of S-O stretching band near 1000 cm^{-1} (Henmi et al., 1981). The bands showed shift toward higher wavenumbers from 428 to 434 cm^{-1} , for KyP and KnP, respectively. The next bands appear at 341 and 347 cm^{-1} for KyP and KnP, respectively. Those bands may be corresponding to the imogolite structure, as reported by Farmer et al. (1977). The band may appear because allophane and imogolite have same basic structure, as described above.

2-2-3 Differential Thermal Analysis

The DTA curves are shown in Fig. 4. The samples generally showed similar features in the DTA pattern, with one broad endothermic and one small exothermic peak. The endothermic peak appears at 90 and 98 °C for KyP and KnP, respectively. The endothermic peak may be arising from continuous dehydration and dehydroxylation (Mitchell et al., 1964; Wada, 1977; Wada, 1989). Furthermore, higher endothermic peak for KnP than KyP sample may correspond to the stronger surface acidity of KnP, sample with high Si/Al ratio (Henmi, 1980). Because, with stronger surface acidity, water molecules are probably more strongly adsorbed as a base on the surface of allophane. In fact, the surface acidity of KnP is higher than that of KyP sample (will be shown at Chapter 4). The exothermic peak appears at 932 and 904 °C for KyP and KnP, respectively. The exothermic peak is attributed to formation of mullite and/or gamma alumina (Mitchell, 1964). The exothermic peak of KnP is higher than that of KyP. This result is consistent with that found by Henmi (1980). The

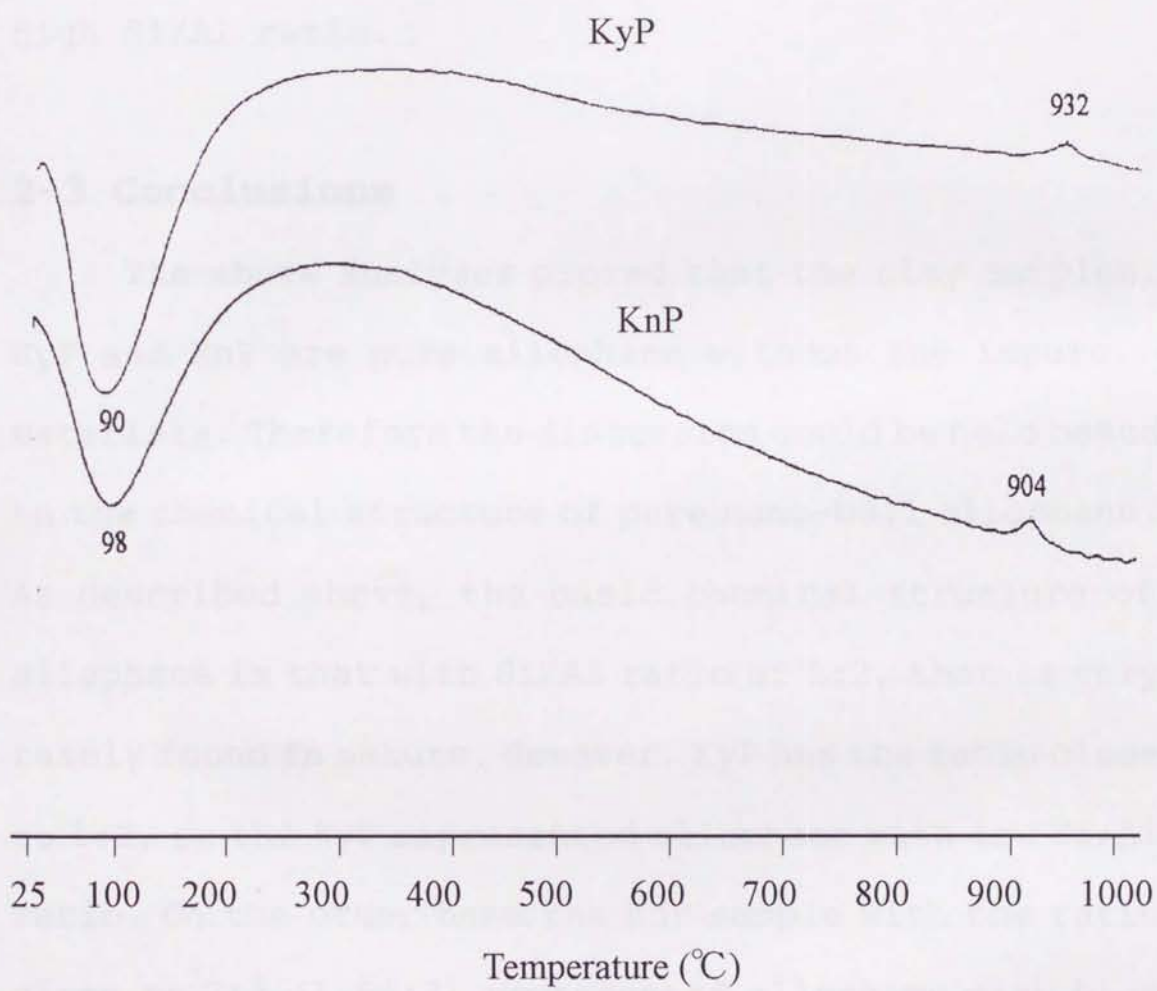


Fig. 4 DTA curves of the allophane samples

difference in the peak position may correspond to the characteristics of samples in relation to the formation of mullite. Henmi (1980) suggested that allophane with low Si/Al ratio is easier to form mullite than that with high Si/Al ratio.

2-3 Conclusions

The above analyses proved that the clay samples, KyP and KnP are pure allophane without any impure materials. Therefore the discussion could be held based on the chemical structure of pure nano-ball allophane. As described above, the basic chemical structure of allophane is that with Si/Al ratio of 1:2, that is very rarely found in nature. However, KyP has the ratio close to 1:2, so the KyP represented allophane with low Si/Al ratio. On the other hand the KnP sample with the ratio close to 2:2 (1.98:2) represented allophane with high Si/Al ratio.

Chapter 3 PHOSPATE ADSORPTION ON ALLOPHANE AND ITS MECHANISM BY MEANS OF MOLECULAR ORBITAL METHOD

3-1 Introduction

Study on phosphate adsorption is important in the views of agriculture and environment. The importance in agriculture is the fact that soils developed from volcanic ash, for example Andepts, are well known to have high phosphorus fixation capacity, showing that large amounts of phosphate fertilizer applied is strongly fixed to them (Sanyal and De Datta, 1991). The property caused problem in agricultural production of that kind of soils, because the phosphate fertilizer is so strongly adsorbed to the soils that the fertilizer become unavailable for plants. Because allophane is the main component of clay materials in Andepts, it was ascribed as the material responsible for the strong adsorption and fixation of phosphate (Wada, 1985). In the view of environment, recently, an issue arose concerning to eutrofication, caused by pouring wastewater containing phosphate in high concentration.

The materials with high capacity for P adsorption such as allophane, may be applied as amendment to solve the problem of eutrofication.

So far, the study of phosphate adsorption were usually focused on soils with relatively high concentrations of phosphate solutions. Hence, the mechanism of phosphate adsorption in soils was not so clear, due to much components in soils, such as organic matters, clay minerals, and ferric or aluminum oxides and hydroxides, which all have ability for P adsorption. On the other hand, not so many researches conducting phosphate adsorption with single clay mineral and at low phosphate concentrations. The advantage of studying P adsorption with single clay mineral is to elucidate the mechanism in detail, based on the chemical structure and characteristics of the mineral.

Based on the above reasons, the study was carried out to understand the clear mechanism of phosphate adsorption on nano-ball shaped allophane samples in relation to its detailed chemical structure. Here, allophane was selected as adsorbent because it has high phosphate adsorption capacity and is the main component

of clays in Andepts. The discussion will be held based on the recently found chemical structure of nano-ball shaped allophane. Molecular orbital calculation was included in this study to elucidate the more detailed mechanism in electron level.

3-2 Materials and Methods

Allophane sample suspensions (KyP and KnP) described in the Chapter 2 were used for the experiment. The suspensions were previously adjusted to pH 5 by adding some drops of HCl solution. About 5 mL of the suspensions containing 50 mg of sample was mixed with NaH_2PO_4 , NaCl, and was filled up with water until total volume of 100 mL. The initial phosphate concentration of the mixed solutions were varied from 0 to 2 mM. The total Na concentration of the mixed solutions were kept as 20 mM by adjusting the amount of NaCl added. The experiment was also done with CaCl_2 background solution, using $\text{Ca}(\text{H}_2\text{PO}_4)_2$ and CaCl_2 , with the initial P concentration up to 2 mM and with 10 mM CaCl_2 .

The mixture was shaken for 20h, then was centrifuged at 7500 rpm to separate precipitated clay

and supernatant. The supernatant was analyzed for pH with pH meter, for P with ascorbic acid method (Murphy and Riley, 1962), for Si by methol sulfite method (Strickland and Parsons, 1968), and for Al by ferron method according to Davenport (1949). Precipitated clay samples were subjected for infrared spectrophotometry and differential thermal analysis after washing with water, in order to observe change in the structure of allophane after the P adsorption. Amount of phosphate adsorbed was calculated from the difference between the initial and final (equilibrium) phosphate concentrations.

For molecular orbital calculation, MOPAC program (Stewart, 1989a) was used with semi-empirical MNDO-PM3 basis set (Stewart, 1989b) which is incorporated in CHAChe system for Windows (CAChe Scientific Inc., Sony Tektronix Corporation). This basis set gives heat of formation closest to experimental values for actual molecules than any other semi-empirical basis sets do (Stewart, 1989b). Cluster models for allophane were built up with Al normal octahedra and Si tetrahedra by using bond distance of Al-O = 0.1912nm, Si-O = 0.1618nm

and O-H = 0.0944nm.

3-3 Results and Discussion

3-3-1 Phosphate Adsorption Isotherm

Figure 5 shows phosphate adsorption isotherms of KyP and KnP samples in NaCl and CaCl₂ background solutions. For all cases, amount of P adsorbed increase with increasing the equilibrium phosphate concentration. The increase is sharp at lower equilibrium P concentration, then the curve gradually become nearly plateau at higher equilibrium phosphate concentrations. However, for all cases further increase in equilibrium phosphate concentration cause irregular increase in amount P adsorbed again. This may be ascribed to destruction or dissolution of allophane due to much amount of phosphate in solution, with results in formation of new aluminol groups (Al-OH or Al-OH₂) at the broken edges. Therefore, for each sample, only the adsorption data until the plateau region will be used for further analysis. Figure 5 shows that KyP sample has higher ability for P adsorption than KnP, either in NaCl or CaCl₂ background solution. This may

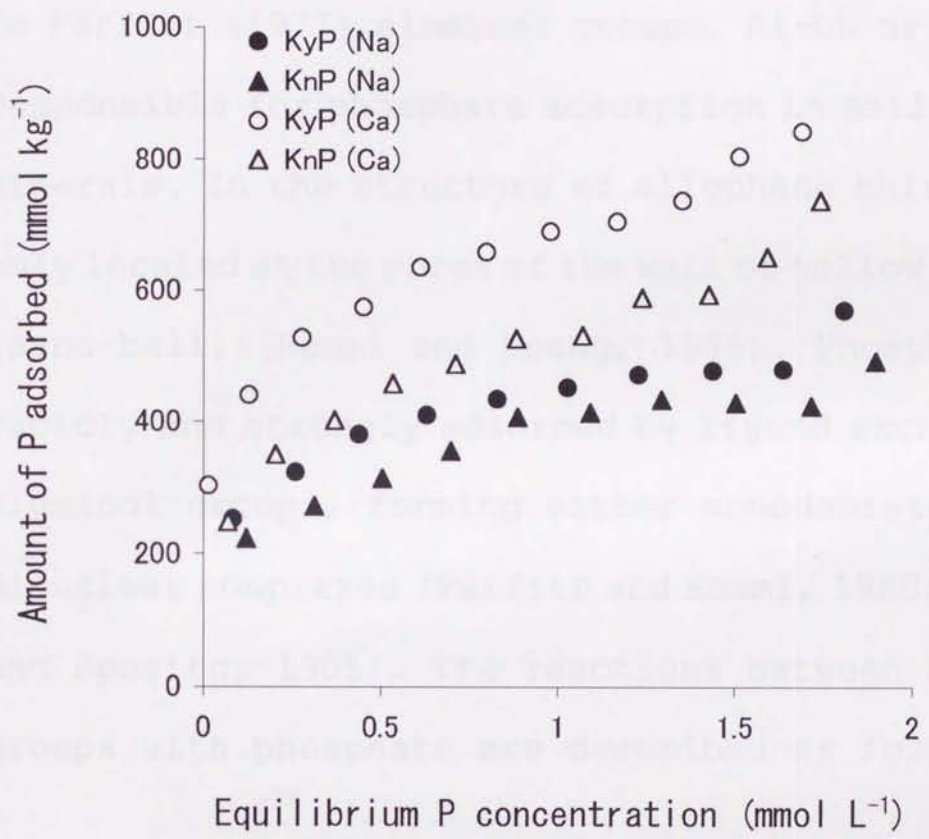
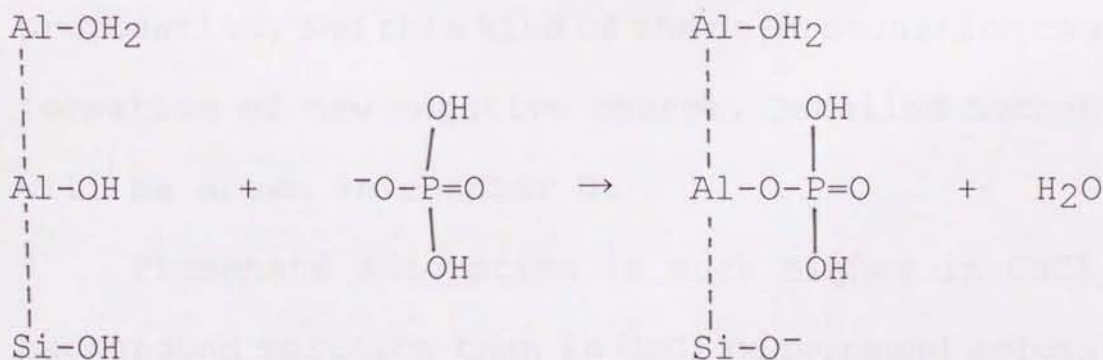
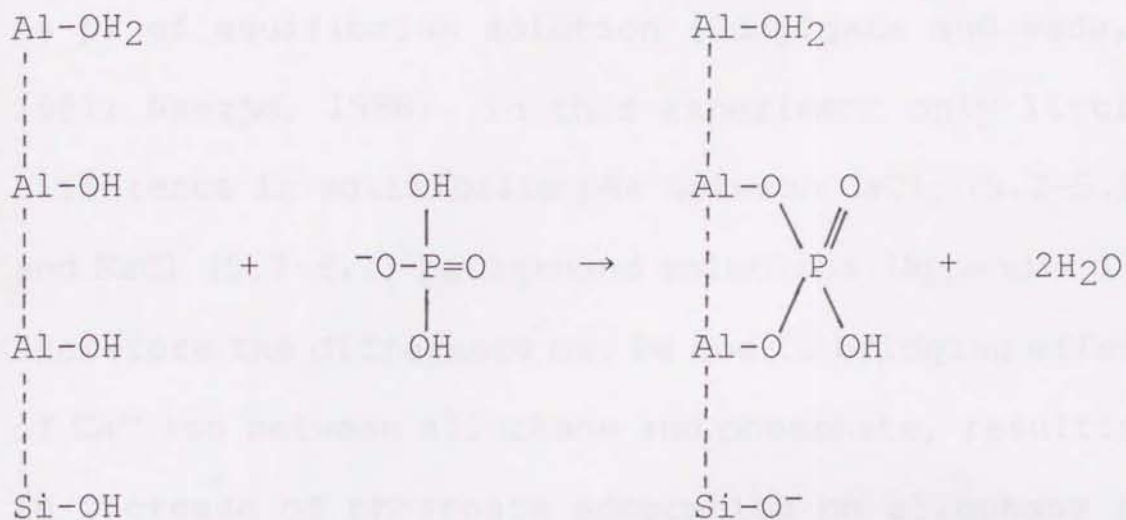


Fig. 5 Phosphate adsorption isotherm of the allophane samples

be ascribed to higher content of Al(OH)(OH)₂ group in the structure of KyP, because KyP has lower Si/Al ratio or greater Al atom contents per unit mass. According to Parfitt (1977) aluminol groups, Al-OH or Al-OH₂ is responsible for phosphate adsorption in soils and clay minerals. In the structure of allophane this group is only located at the pores of the wall of hollow spherules (nano-ball) (Henmi and Huang, 1985). Phosphate is rapidly and strongly adsorbed by ligand exchange with aluminol groups, forming either monodentate or binuclear complexes (Parfitt and Henmi, 1980; Goldberg and Sposito, 1985). The reactions between aluminol groups with phosphate are described as follow:





The above reactions describe reaction of phosphate with one aluminol, and that with two aluminols, respectively. The reactions resulted in formation of monodentate and binuclear complexes, respectively. The bottom Si-OH is the silanol group nearby allophane-phosphate adsorption complex. The silanol group undergoes deprotonation, and this kind of the deprotonation causes formation of new negative charge. Detailed mechanism will be shown in chapter V.

Phosphate adsorption is much higher in CaCl_2 background solution than in NaCl background solution, for both KyP and KnP samples. It is known that amount of phosphate adsorbed on allophanic clays is affected

by pH of equilibrium solution (Gunjigake and Wada, 1981; Nanzjo, 1988). In this experiment only little difference in equilibrium pHs between CaCl_2 (5.2-5.9) and NaCl (5.7-6.1) background solutions (Appendix 1). Therefore the difference may be due to bridging effect of Ca^{2+} ion between allophane and phosphate, resulting in increase of phosphate adsorption on allophane in CaCl_2 background solution. The bridge could be described as phosphate (H_2PO_4^-) which is bonded to the Ca^{2+} cations in the surface of allophane, as described below. Here, the phosphate is not bonded directly to the aluminol groups.

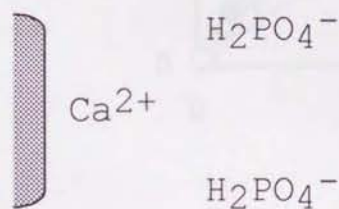


Fig. 5 Langmuir isotherm for adsorption of phosphate by the samples

3-3-2 Langmuir Adsorption Equation

The phosphate adsorption data were plotted according to Langmuir adsorption equation. Figure 6 shows those curves, which two straight lines obtained for all cases, up to equilibrium phosphate

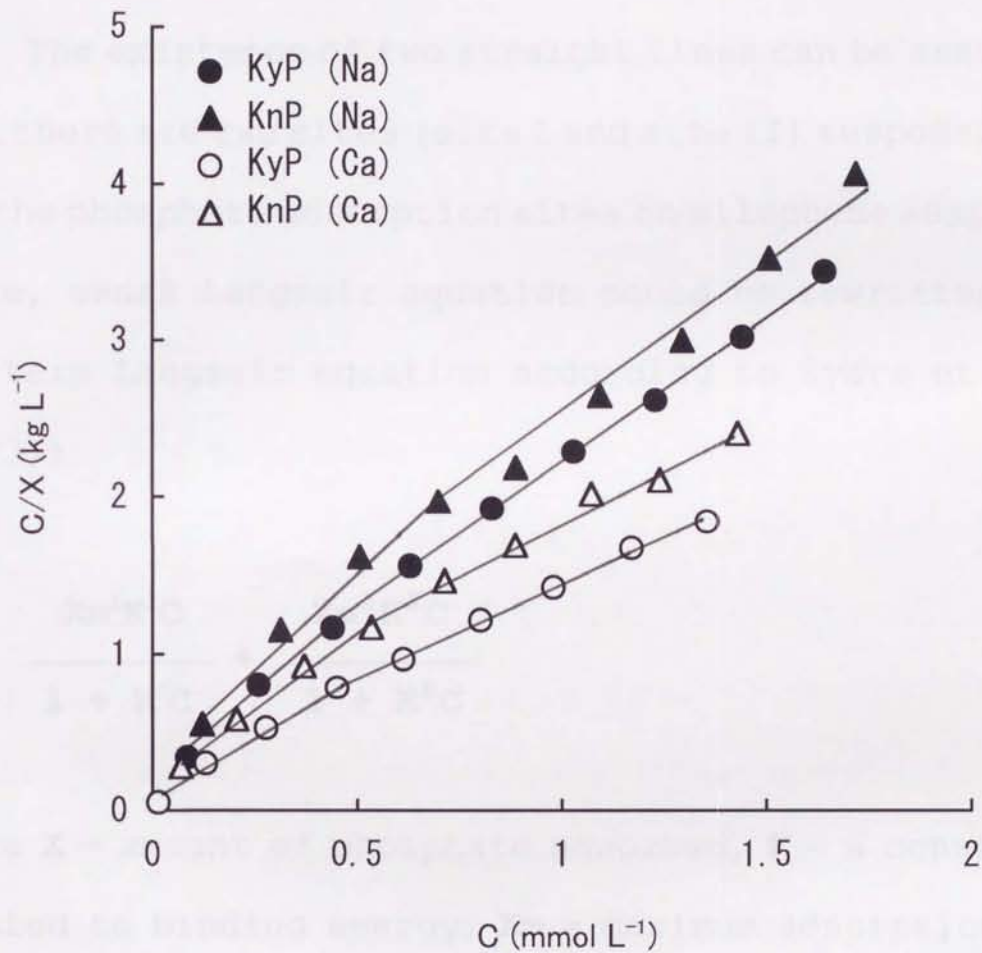


Fig. 6 Langmuir isotherm for adsorption of phosphate by the samples.

C: equilibrium P concentration (mmol L⁻¹), X: amount of P adsorbed (mmol kg⁻¹)

concentration of 1.5 to 1.8 mM, for KyP and KnP samples, respectively. The break of the two straight lines existed at the equilibrium phosphate concentration of about 0.4 to 0.5 mM, for the all cases.

The existence of two straight lines can be assumed that there are two sites (site I and site II) responsible for the phosphate adsorption sites on allophane samples. Hence, usual Langmuir equation could be rewritten as two-term Langmuir equation according to Syers et al. (1973):

$$X = \frac{X_m^I K^I C}{1 + K^I C} + \frac{X_m^{II} K^{II} C}{1 + K^{II} C} \quad (1)$$

where X = amount of phosphate adsorbed, K = a constant related to binding energy, X_m = maximum adsorption of phosphate, and C = equilibrium phosphate concentration. The superscripts I and II refer to site I and site II, respectively. The X_m^I and K^I values were calculated from data at lower C values (up to break point) by assuming all of the phosphate were adsorbed on site I, then each amount of phosphate adsorbed due to site I, X^I was

calculated for all C values. The X^{II} value was obtained by subtracting X^I from X at each C value, then Xm^{II} and K^{II} were calculated.

Table 1 gives so calculated Langmuir parameters, and indicates (both samples and cation species) Xm^I and K^I were greater than corresponding Xm^{II} and K^{II} , respectively. The data indicate that site I is twice to three times higher in phosphate adsorption capacity than the site II, and that the site I has binding energy for phosphate more than 10 times greater than the site II. Even in solution, allophane is known to form aggregates with many unit particles, creating outer and inner surfaces on and in the aggregates (Wada, 1989). The inner surface in the aggregates may correspond to the site I, while the outer surface on the aggregates correspond to the site II. As mentioned above, the phosphate adsorption reaction is ascribed to the aluminol groups, located in the pores or defect of the structure of allophane (Henmi and Huang, 1985).

Phosphate may first react with aluminol groups inside the aggregates (site I), since the site I has greater adsorption energy than the site II, then

Table 1 Adsorption maxima (X_m) and binding energy constants (K) of the allophane samples

Sample	Site I		Site II		X_m^I	K^I
	X_m^I	K^I	X_m^{II}	K^{II}	X_m^{II}	K^{II}
NaCl background solution						
KyP	432	14.3	116	1.0	3.7	14.3
KnP	357	11.8	108	3.1	3.3	3.8
CaCl ₂ background solution						
KyP	601	32.2	295	2.6	2.0	12.6
KnP	438	25.6	196	1.2	2.2	22.1

X_m : mmol kg⁻¹; K : (mM)⁻¹

phosphate react with aluminol groups at the outer surface on aggregates (site II), after saturating the site I.

3-3-3 Silicon Release

In the P adsorption experiments, Si and Al were always detected in the equilibrium solution after the phosphate adsorption under the present condition, for the all cases. Figure 7 gives relationship between the amount of phosphate adsorbed and Si or Al released for KyP and KnP in NaCl and CaCl₂ background solutions. The amount of Si released increased linearly with increasing amount of phosphate adsorbed, for both samples and both cation species. On the other hand, the amounts of Al released were much lower than Si released, for the all cases. The slopes of the plots for Si were calculated as 0.13 and 0.34 for KyP and KnP, respectively in Na background solution and as 0.16 and 0.40 for KyP and KnP, respectively in Ca background solution. The linear relationships as the Si released, were not observed for the Al released. The release of Al may be due to small dissolution from allophane

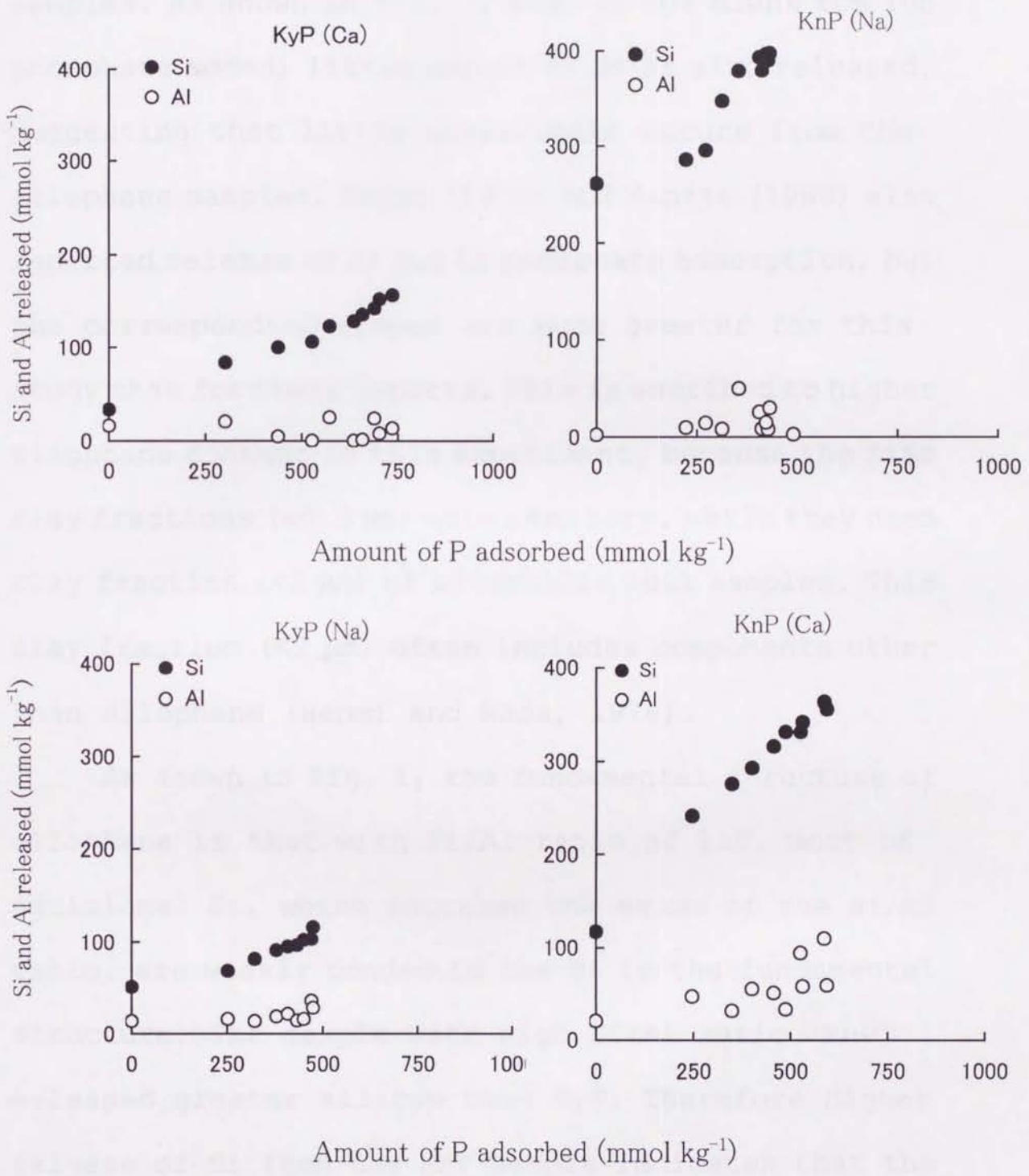


Fig. 7 Relationship between the amount of P adsorbed and the amount of Si and Al released of the allophane samples

samples. As shown in Fig. 7, even in the blank run (no phosphate added) little amount of Si is also released, suggesting that little dissolution occurs from the allophane samples. Rajan (1975) and Nanzjo (1988) also reported release of Si due to phosphate adsorption, but the corresponding slopes are much greater for this study than for their reports. This is ascribed to higher allophane content in this experiment, because the fine clay fractions ($<0.2 \mu\text{m}$) were used here, while they used clay fraction ($<2 \mu\text{m}$) of allophanic soil samples. This clay fraction ($<2 \mu\text{m}$) often includes components other than allophane (Henmi and Wada, 1976).

As shown in Fig. 1, the fundamental structure of allophane is that with Si/Al ratio of 1:2. Most of additional Si, which increase the value of the Si/Al ratio, are weakly bonded to the Si in the fundamental structure. The sample with high Si/Al ratio (KnP) released greater silicon than KyP. Therefore higher release of Si from the KnP sample indicates that the weakly bonded Si is replaced by phosphate, rather than that Si attached to gibbsite sheet in the structure of allophane. The linearity in Fig. 7 suggests that in a

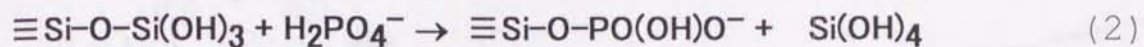
unit particle of allophane, the replacement reaction takes place simultaneously with adsorption of phosphate on aluminol groups, over the whole range of equilibrium phosphate concentrations. Ratio of (phosphate adsorbed by Si replacement)/(total phosphate adsorbed) is roughly estimated as 0.13 and 0.34 for KyP and KnP, respectively, in Na background solution. The ratio is estimated as 0.16 and 0.40 for KyP and KnP, respectively, in Ca background solution. That ratio is calculated by assuming that one phosphate replaces one weakly bonded Si.

3-3-4 Molecular Orbital Analysis

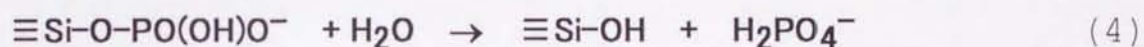
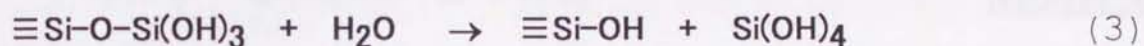
The obtained experimental results indicated that the phosphate adsorption reaction on unit particle of nano-ball allophane included reaction in Al and in Si. The reaction of phosphate in Al has been known well not only for allophanic clays, but also in other kind of clays. Nevertheless, relatively lack information for reaction of phosphate in Si, which is reported until now.

The possible reaction for displacement of weakly

bonded Si with P is formulated as:

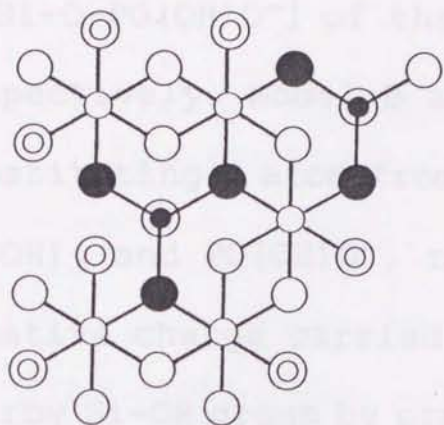


The [$\equiv\text{Si}$] is the silicon directly bonded to gibbsite sheet on the structure of allophane, and exists as Si-OH in allophane with Si/Al ratio of 1:2. The equation (2) could be obtained by combination of following two reactions:

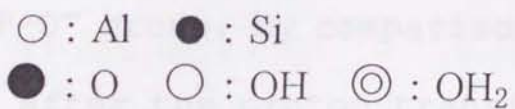
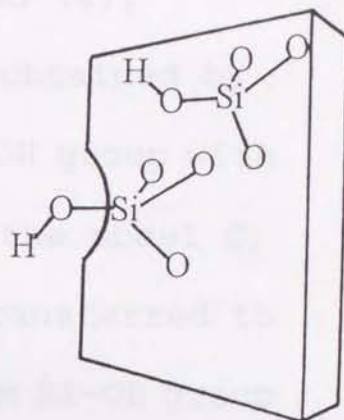


The equation (3) and (4) describe hydrolysis reaction of silicic acid and phosphate adsorbed on fundamental structure of allophane (Si/Al = 1:2), respectively. The possibility of the replacement reaction was analyzed by molecular orbital method. Heat of formation was calculated for each molecule, then change in heat of formations (ΔH) were calculated for each equation. Here, $\Delta H = H_{\text{products}} - H_{\text{reactants}}$, and lower ΔH of a reaction indicates that the reaction is more possible.

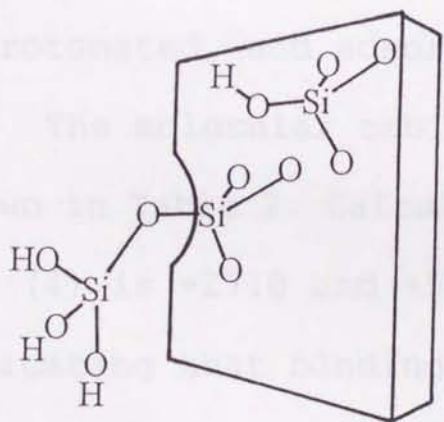
Figure 8 shows model clusters used for the molecular orbital calculation. Model A simulates model cluster for the ($\equiv\text{Si-OH}$) of the equation 2. Model B



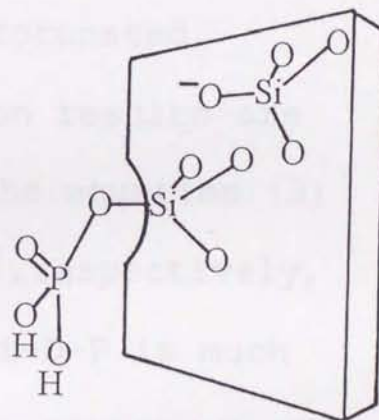
=



Model A



Model B



Model C

Fig. 9 Model clusters of allophane used for molecular orbital calculation

and model C are model clusters for $[\equiv\text{Si-O-Si(OH)}_3]$ and $[\equiv\text{Si-O-PO(OH)O}^-]$ of the equation (3) and (4), respectively. Model B and model C were obtained by substituting H atom from the central Si-OH group with Si(OH)_3 and PO(OH)O^- , respectively. In the model C, negative charge carried by H_2PO_4^- was transferred to nearby Si-OH group by proton transfer from Si-OH group to P-O^- group. By comparison heat of formation before and after the proton transfer (data will be shown at chapter V), it is indicated that the proton transfer stabilized model C, with the result, Si-OH group is deprotonated, and adsorbed P-O^- is protonated.

The molecular orbital calculation results are shown in Table 2. Calculated ΔH for the equation (3) and (4) is +27.8 and +51.5 kcal mol⁻¹, respectively, indicating that binding energy of $\equiv\text{Si-O-P}$ is much stronger than that of $\equiv\text{Si-O-Si}$ in the structure of nano-ball allophane. The equation (2) can be obtained by subtracting equation (4) from equation (3). The calculated ΔH for the equation (1) is -23.7 kcal mol⁻¹. The negative value indicates that the equation (1), replacement of weakly bonded Si with P, is possible.

3-3-5 Change in Aliphatic Structure after the P

Adsorption

Table 2 Calculated ΔH (change in heat of formation) for equations (2), (3) and (4)

Equation	ΔH (kcal mol ⁻¹)
(2) $\equiv\text{Si-O-Si(OH)}_3 + \text{H}_2\text{PO}_4^- \rightarrow \equiv\text{Si-O-PO(OH)O}^- + \text{Si(OH)}_4$	-23.7
(3) $\equiv\text{Si-O-Si(OH)}_3 + \text{H}_2\text{O} \rightarrow \equiv\text{Si-OH} + \text{Si(OH)}_4$	+27.8
(4) $\equiv\text{Si-O-PO(OH)O}^- + \text{H}_2\text{O} \rightarrow \equiv\text{Si-OH} + \text{H}_2\text{PO}_4^-$	+51.5

3-3-5-1 Differential Thermal Analysis

DTA patterns after the P adsorption were presented in Fig. 9 and Fig. 10, for the KyF and Knp samples, respectively. The patterns tend to be similar each other, before and after the P adsorption. All of the patterns showed one endothermic peak around 90-100°C and one exothermic peak around 300°C. However, for the KyF samples, the endothermic peak shifted to higher region, at high range of P adsorption. This may have relationship with surface acidity. With increasing the

3-3-5 Change in Allophane Structure after the P

Adsorption

The allophane samples were subjected for analysis with IR spectroscopy and with DTA, after the P adsorption, to know possible change in their structure. The analysis were carried out for the samples with Ca background solutions, due to the sample resulted higher amount of P adsorbed, than that with Na background solutions. X-ray diffractograms were not shown, since no change was observed for the allophane samples before and after the P adsorption.

3-3-5-1 Differential Thermal Analysis

DTA patterns after the P adsorption were presented in Fig. 9 and Fig. 10, for the KyP and KnP sample, respectively. The patterns tend to be similar each other, before and after the P adsorption. All of the patterns showed one endothermic peak around 90-100°C and one exothermic peak around 900°C. However, for the KyP samples, the endothermic peak shifted to higher region, at high range of P adsorption. This may have relationship with surface acidity. With increasing the

KyP

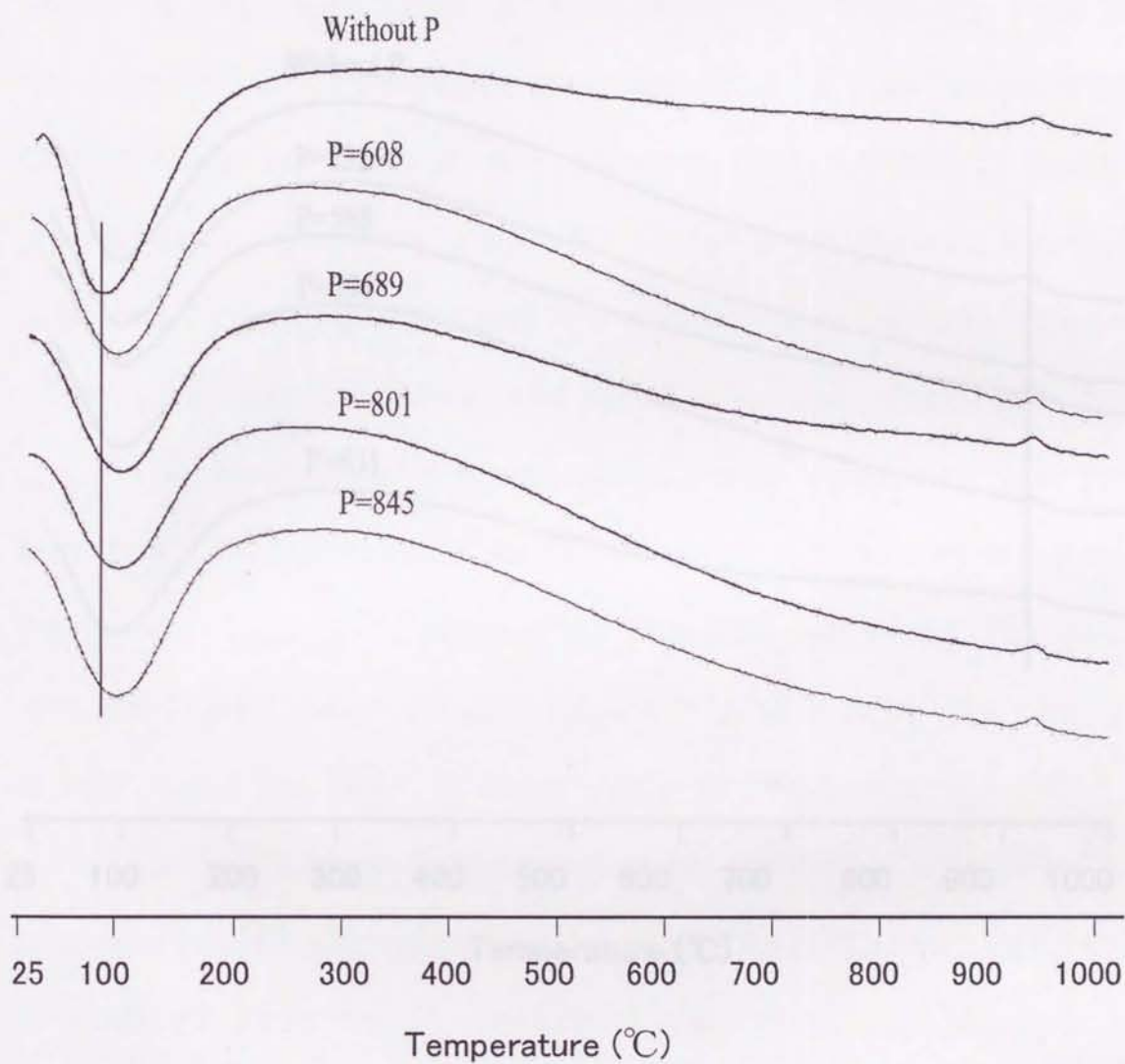


Fig. 9 DTA curve of the KyP sample before and after the P adsorption (amounts of P adsorbed are expressed in mmol kg^{-1})

KnP

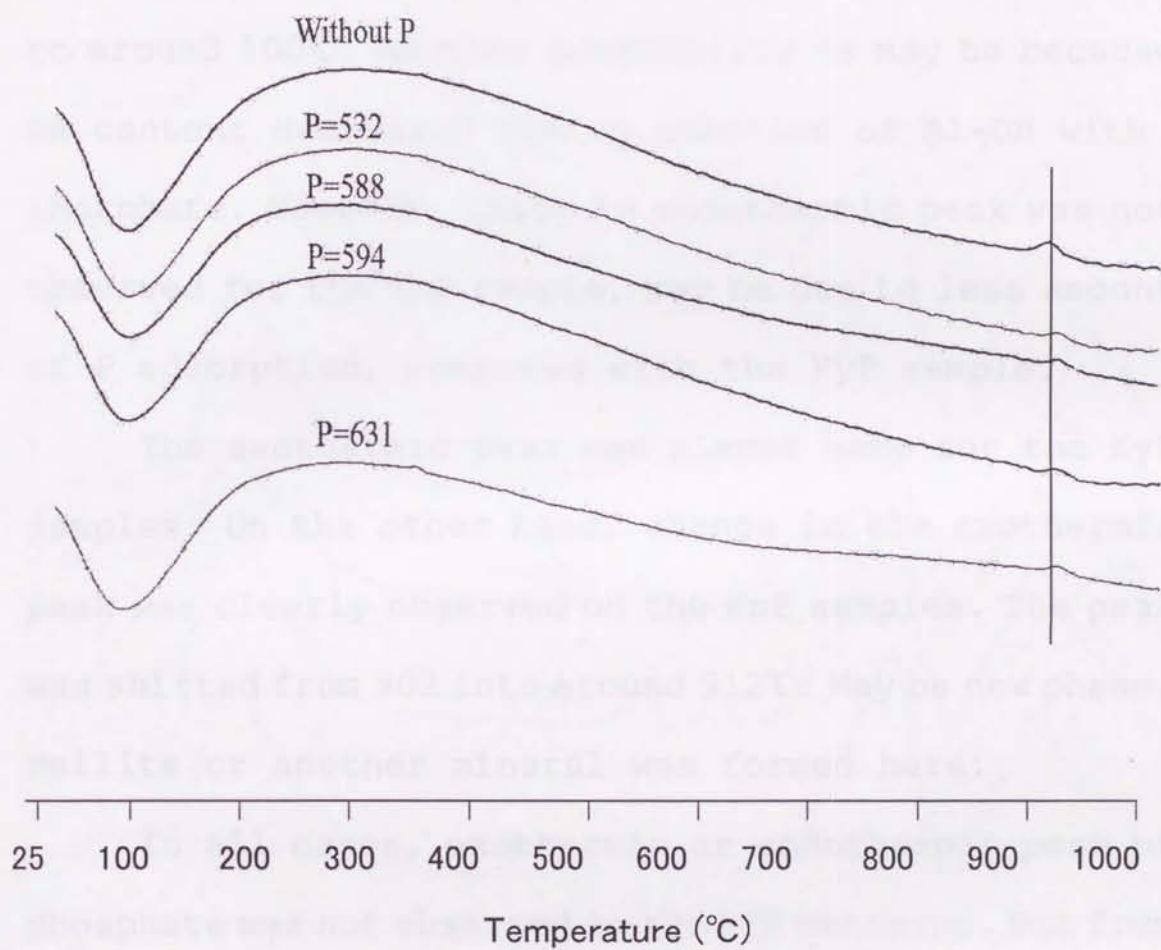


Fig. 10 DTA curve of the KnP sample before and after the P adsorption
(amounts of P adsorbed are expressed in mmol kg^{-1})

surface acidity may be much more water are adsorbed as base on the surface of allophane, with the results the endothermic peak shifted to the higher region, from 90 to around 100°C. Another possibility is may be because OH content decreased due to reaction of Al-OH with phosphate. However, shift in endothermic peak was not observed for the KnP sample, may be due to less amount of P adsorption, compared with the KyP sample.

The exothermic peak was almost same for the KyP samples. On the other hand, change in the exothermic peak was clearly observed on the KnP samples. The peak was shifted from 902 into around 912°C. May be new phase, mullite or another mineral was formed here.

In all cases, exothermic or endothermic peak of phosphate was not observed in the DTA patterns. But from the above results it is concluded that the phosphate adsorption might influence physico-chemical properties of allophane.

3-3-5-2 Infrared Spectroscopy

Infrared spectra were shown at Fig. 11 and Fig. 12 for KyP and KnP, respectively.

KyP

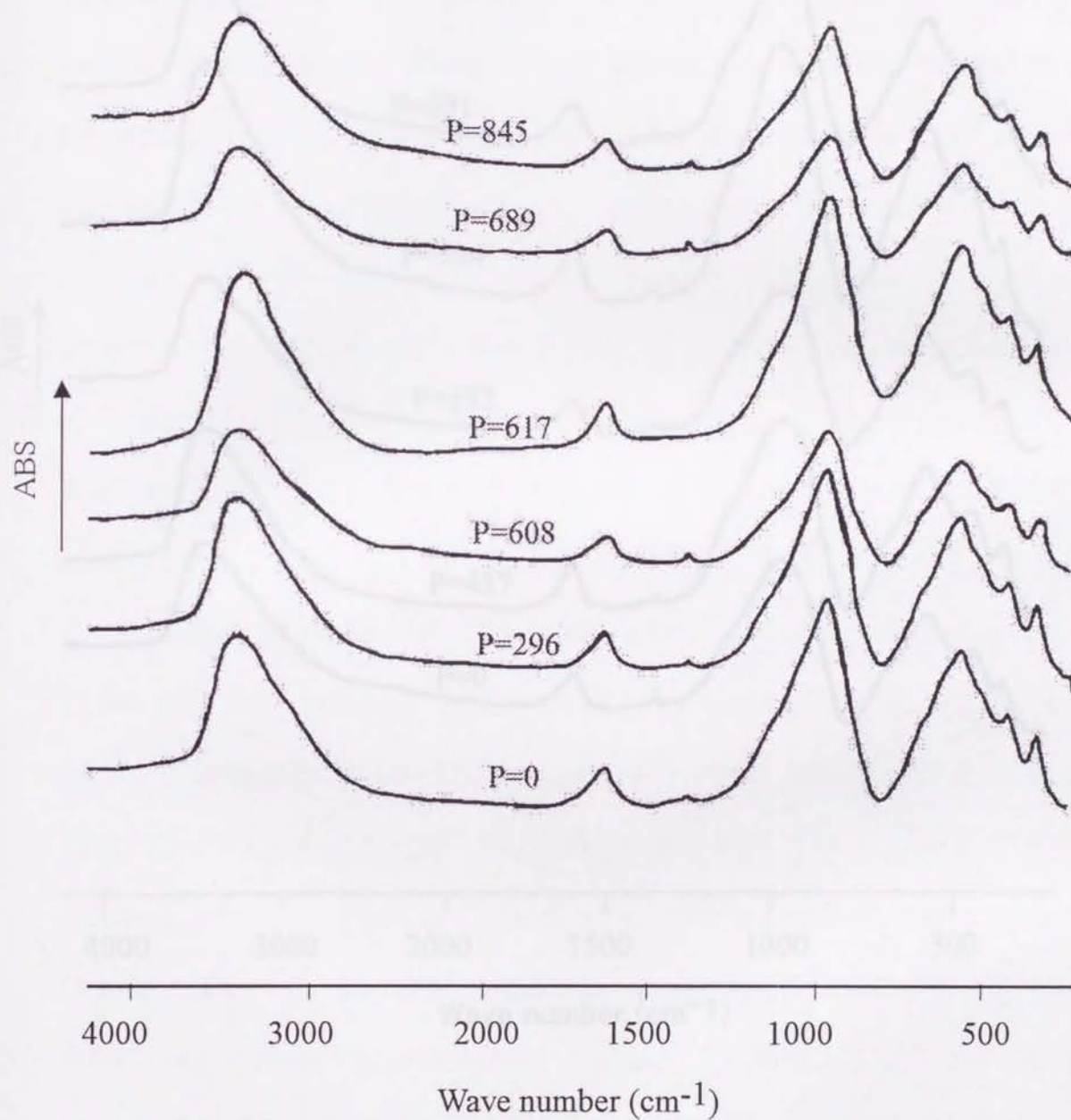


Fig. 11 Infrared spectra of KyP at various amounts of P adsorbed (the figure expressed amounts of P adsorbed in mmolkg⁻¹)

KnP

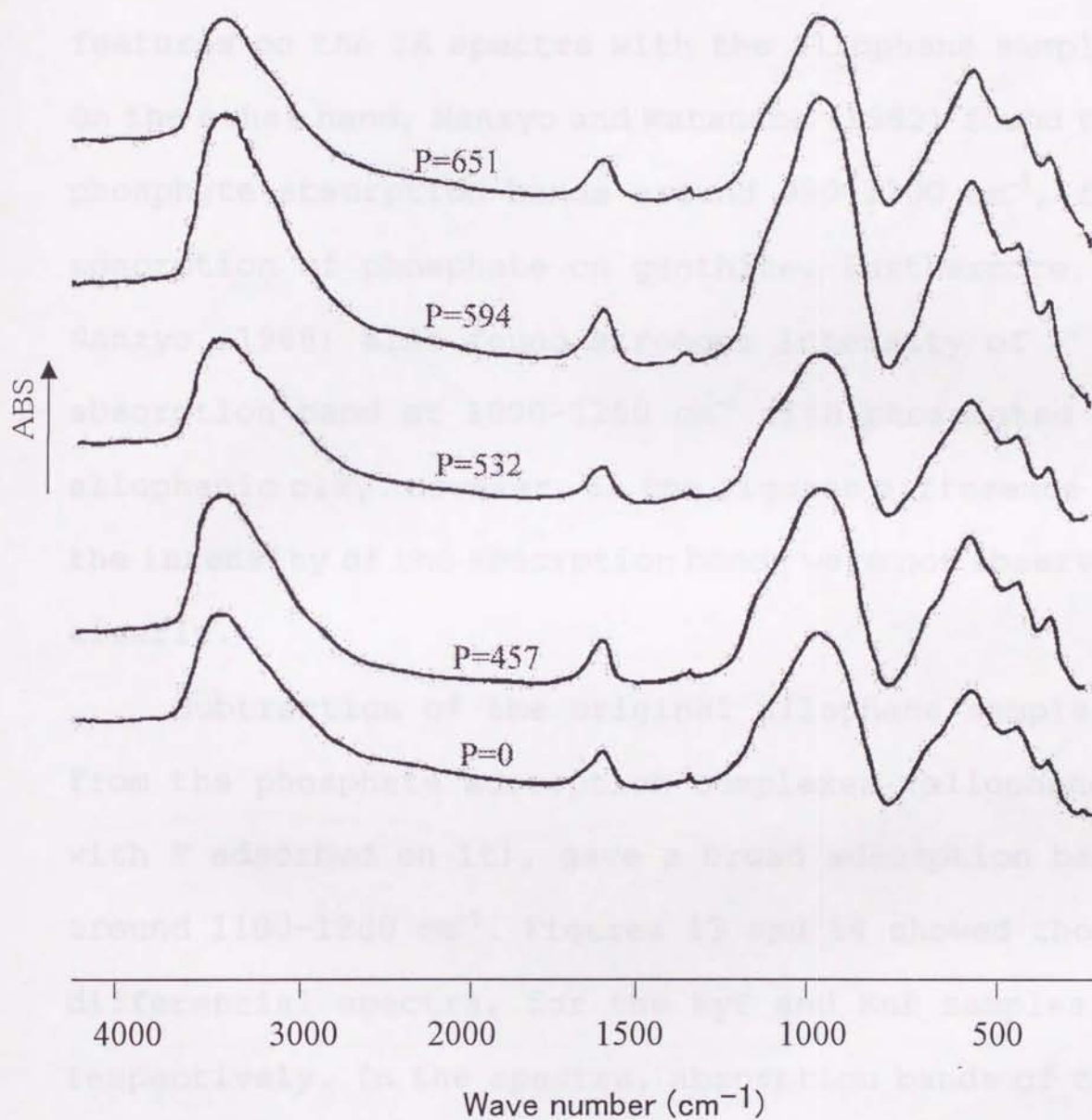


Fig. 12 Infrared spectra of KnP at various amounts of P adsorbed (the figure expressed amounts of P adsorbed in mmolkg⁻¹)

Generally, phosphate adsorption complexes (allophane with phosphate adsorbed on its structure) give similar features on the IR spectra with the allophane sample. On the other hand, Nanzyo and Watanabe (1982) found two phosphate absorption bands around $990-1200\text{ cm}^{-1}$, for adsorption of phosphate on goethite. Furthermore, Nanzyo (1988) also found stronger intensity of absorption band at $1000-1250\text{ cm}^{-1}$ with phosphated allophanic clay. However, in the figures difference in the intensity of the absorption bands were not observed clearly.

Subtraction of the original allophane samples from the phosphate adsorption complexes (allophane with P adsorbed on it), gave a broad adsorption band around $1100-1200\text{ cm}^{-1}$. Figures 13 and 14 showed those differential spectra, for the KyP and KnP samples, respectively. In the spectra, absorption bands of the adsorbed phosphate appear around 1120 to 1147 cm^{-1} and around 1112 to 1207 cm^{-1} for the KyP and KnP samples, respectively. The position of the bands varied with amount of P adsorbed. The absorption bands may be due to P-O stretching vibration of the sorbed phosphate.

KyP

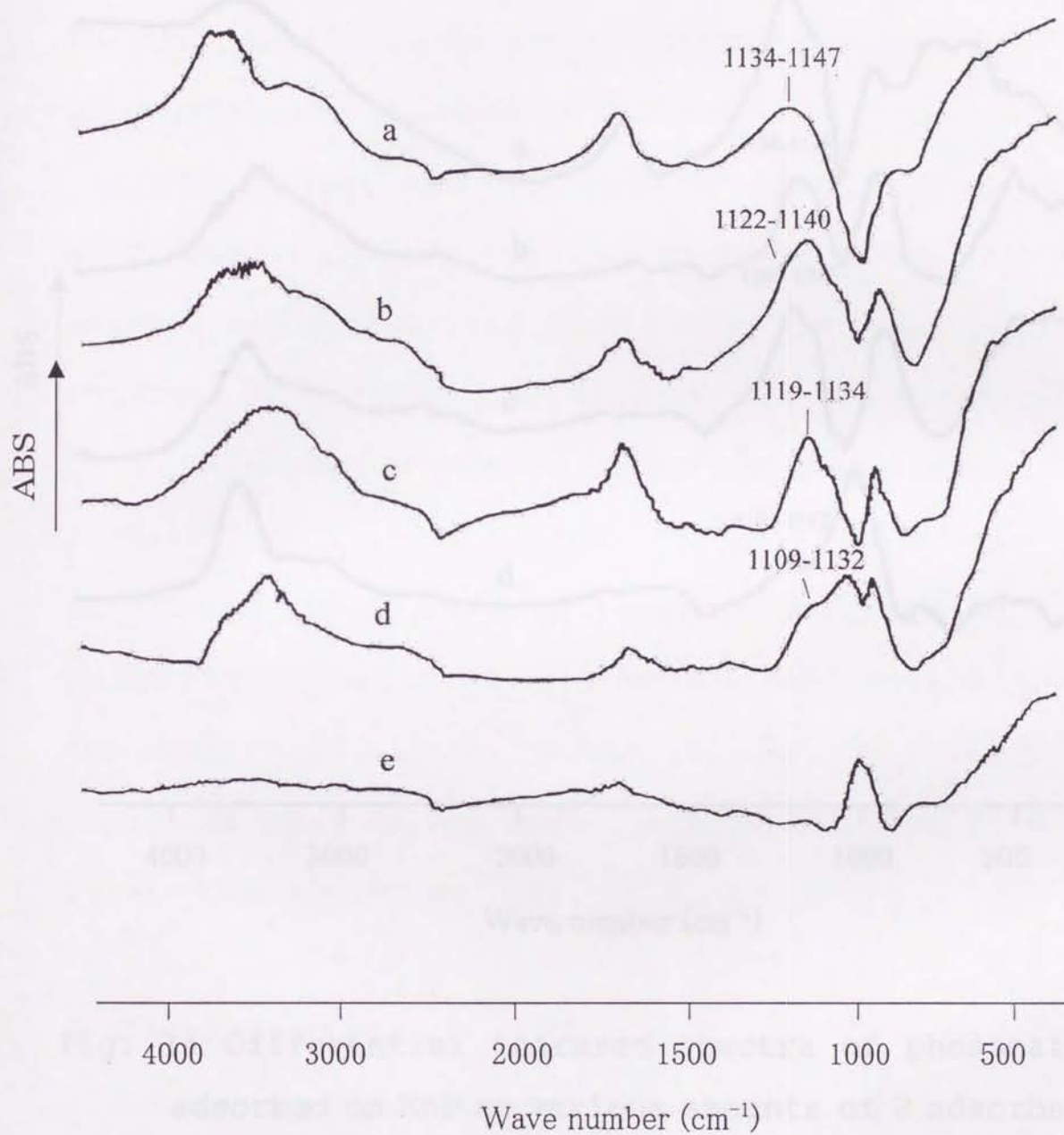


Fig. 13 Differential infrared spectra of phosphate adsorbed on KyP at various amounts of P adsorbed (a:845; b:869; c:617; d:608; e:296 mmolkg⁻¹)

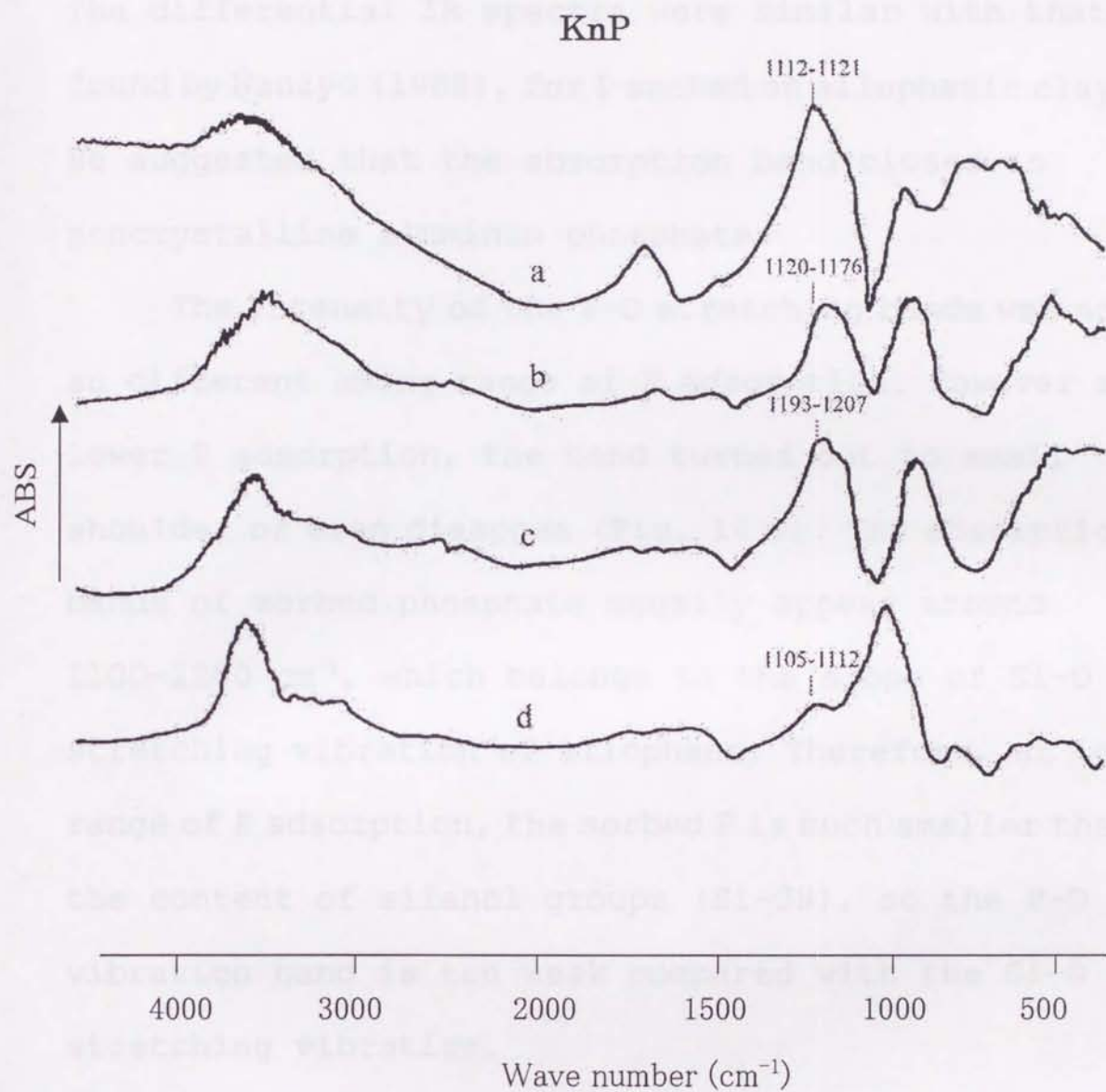


Fig. 14 Differential infrared spectra of phosphate adsorbed on KnP at various amounts of P adsorbed (a:651; b:594; c:532; d:457 mmolkg^{-1})

The differential IR spectra were similar with that found by Nanzyo (1988), for P sorbed on allophanic clay. He suggested that the absorption band closed to noncrystalline aluminum phosphate.

The intensity of the P-O stretching bands was not so different among range of P adsorption. However at lower P adsorption, the band turned out to small shoulder or even disappear (Fig. 14 e). The absorption bands of sorbed phosphate usually appear around 1100-1200 cm^{-1} , which belongs to the slope of Si-O stretching vibration of allophane. Therefore, at low range of P adsorption, the sorbed P is much smaller than the content of silanol groups (Si-OH), so the P-O vibration band is too weak compared with the Si-O stretching vibration.

3-4 Conclusions

1. A new mechanism, replacement of weakly bonded Si with P, is proposed for phosphate adsorption on nano-ball shaped allophane. This is one kind of chemical reaction between allophane and phosphate.
2. High concentration of phosphate in aqueous solution

caused partial dissolution of chemical structure of allophane. The critical equilibrium phosphate concentration is about 1.5 to 1.8 mM.

3. The presence of Ca^{2+} ion enhanced the phosphate adsorption on allophane, probably by bridging effect of the ion between allophane and phosphate.
4. Structure of allophane is not ruptured up to initial P concentration of 2 mM, at least proved by features in IR and DTA.

Chapter 4 CHANGE IN SURFACE ACIDITY OF ALLOPHANE

WITH P ADSORPTION

4-1 Introduction

Solid surface is known to have acidic properties, called surface acidity. The acidity of solid surface is proved by its ability to catalyze some organic reactions such as polymerization reaction. For example, kaolinite has known to have ability to catalyze polymerization of styrene and other monomers susceptible to cationic polymerization (Solomon 1968; Solomon and Murray, 1971). Attapulgite and montmorillonite were also known to have ability as catalysts (Solomon, 1968). The ability is due to the clay minerals act as electron acceptor. Other kind of clay minerals are also known to have surface acidity, such as pyrophyllite, talc, allophane, and imogolite (Solomon, 1968, Henmi and Wada, 1974; Wu et al., 1992; Henmi et al., 1997). However, there are lack in information concerning characteristics of the surface acidity in detail for those clays. The information concerning the surface acidity of clays, is important

to understand their surface properties. Furthermore, the insight can be developed and be applied for much purpose in agriculture, chemical engineering, or environmental fields.

The acid strength of a solid is defined as ability of a surface to convert an adsorbed neutral base into its conjugate acid (Walling, 1970). The acid strength is expressed as follow:

$$H_o = -\log a_{H^+} f_B / f_{BH^+}$$

or

$$H_o = pK_a + \log [B] / [BH^+]$$

Where a_{H^+} is the proton activity, [B] and $[BH^+]$ are the concentration of the neutral base and its conjugate acid, respectively, and f_B and f_{BH^+} are the corresponding activity coefficients.

The origin of acidity of solid surface consists of Lewis acidity as electron acceptor and Brønsted acid as proton donor. Brønsted acidity is defined as the ability of a molecule to give up a proton (Siggel et al., 1988), while Lewis acidity is the ability of a molecule to accept an electron. Brønsted acidity origins from exchangeable hydrogen, water adsorbed on

exchangeable cations, and from dissociation of functional groups, while Lewis acidity origins from exchangeable cations on permanent negative charge and from unsaturated structural silicon or aluminum (Wu et al., 1992).

The acid strength and number of the surface acidity are influenced by relative humidity and cation type saturating over clay surface. For example, the acidity of H-allophane (hydrogen saturated allophane) or H-montmorillonite, is stronger than that of Ca-montmorillonite or Ca-allophane, respectively (Henmi and wada, 1974). The effect of exchangeable cation is influenced by polarization, that is determined by ratio of number of charge per diameter ion, which greater that ratio causes stronger the acidity (Tanabe, 1970; Henmi and Wada, 1974).

Brønsted acidity is possibly to convert into Lewis acidity, and vice versa. For example, strong acid of a mineral surface caused by exchangeable calcium (Lewis acidity) will change into weaker acidity (Brønsted acidity) if it adsorbs water. Saturation treatment with alkali or alkaline earth metals on a clay was known to

eliminate all of Brønsted acidity of the clay surface and remain only Lewis acidity (Shephard et al., 1962; Hawthorne and Solomon, 1972). However, a weak Brønsted acidity will appear again by adsorption of water molecule (increase in relative humidity) on the exchangeable alkali or alkaline earth metal ions.

As described earlier, the acidity of clay minerals plays important role in some polymerization reactions, due to their ability as proton acceptor. Recently, in the field of agriculture and environment, attentions are also paid to the surface acidity of clay minerals. This because the surface properties of clay minerals plays important role in determining its physico-chemical characteristics, that is important for its application in agriculture or environmental views. The other reason is because all of chemical reaction occurs at the surface of clay minerals. It was expected that acid sites of some clay minerals acted as cation exchange site in the pH range, which is normally found in soils (Henmi and Wada, 1974).

Allophane, the main clay components in Andepts, has acidity stronger than imogolite, but weaker than

montmorillonite and kaolinite. Functional groups on the structure of allophane, Si-OH and Al-OH, may act as Brønsted acid sites. The study concerning acid strength and acid sites of allophane has been studied intensively by Henmi and Wada (1974). The acidity of allophane is also affected by kind of saturating cation and relative humidity.

The acidity of allophane with low Si/Al ratio, was increased by adsorption of orthosilicate, due to enhancement in the Brønsted acidity of the silanol groups on the structure of allophane (Henmi et al., 1997). The similar results were also observed for adsorption of flourine on allophane (Henmi et al., 1998). On the other hand, the CEC of allophane also increased due to phosphate adsorption (Nanzyo, 1988) and flourine adsorption (Henmi et al., 1998). Based on the above results, it is expected that surface acidity of allophane can be changed by phosphate adsorption. The objectives of the study is to know change in characteristics of surface acidity of allophane induced by P adsorption, and to elucidate its mechanism. The results will provide information to get more

insight in the surface structure of allophane.

4-2 Materials and Methods

The allophane samples as described earlier, were used for the surface acidity experiment. The samples were previously treated with DCB (dithionite citrate bicarbonate) twice, for iron removal according to Mehra and Jackson method (1960). The treatment was purposed to change the color of samples from reddish into white, because the measurement in the surface acidity was judged by naked eyes, and many indicators with red color were used.

Phosphate adsorption was carried out as follow. About 150 mg of allophane sample was mixed with 2 to 20 mL of 30 mM of NaH_2PO_4 , then pure water was added, in order to fill up until 300 mL. The mixtures gave a series of suspension with initial P concentration ranged from 0.2 to 2 mM. The mixtures were shaken for 20 h, then were centrifuged. Separated clay samples were washed once with water then were dried in air. The supernatant was analyzed for P with ascorbic acid method as described earlier. Part of clay samples (with

and without P adsorption) were treated with H^+ saturated resin in order to exchange Na into H saturation, then were followed by washing with pure water, to remove excess of H^+ . All of the samples were heated at $105\text{ }^\circ\text{C}$ for 6 h, then were equilibrated under various relative humidity (RH) sets. To give desired a relative humidity, saturated salts solution was put in a desiccator, then was kept to stand it for several hours. For example, sodium carboxylate ($\text{CH}_3\text{COONa}\cdot 3\text{H}_2\text{O}$) saturated solution gives relative humidity of 76%.

Acid strength was measured for each sample at various RH sets and after heating at $105\text{ }^\circ\text{C}$ according to the method of Walling (1950) and Benesi (1956). The acid strength of the samples was estimated from the color of Hammet indicators (H_0) having known pK_a . Table 3 shows the indicator used for the surface acidity measurement. The concentration of each indicator was 1%, dissolved in benzene solution. The acidity (H_0) was expressed with ordinary number from rank I to rank VI, as shown in table 4.

After equilibrating samples under various RHs, about two drops indicator solution was added to the

Table 3 List of Hammet indicators used for the surface acidity measurement

Indicator	Color		pKa	H ₂ SO ₄ ^{a)} (wt %)
	Basic	Acidic		
4'-Dimethylaminoazobenzene-2-carboxylic acid (Methyl red)	Yellow	Red	5.0	-
4-Phenylazo-1-naphthylamine (Naphthyl red)	Yellow	Purple	4.0	5X10 ⁻⁵
N,N-Dimethyl-4-(phenylazo)-Benzenamine (Butter yellow)	Yellow	Red	3.3	3X10 ⁻⁴
2-Methyl-4-[(2-methylphenyl)-azo] benzenamine (o-aminoazotoluene)	Yellow	Red	2.0	5X10 ⁻³
4-Phenylazodiphenylamine (4-Benzenazodiphenylamine)	Yellow	Purple	1.5	2X10 ⁻²
1,9-Diphenyl-1,3,6,8-nonatetraene-5-one (Dicinnamalacetone)	Yellow	Red	-3.0	48
1,3-Diphenyl-2-propene-1-one (Benzalacetophenone)	Colorless	Yellow	-5.6	71

a) Sulfuric acid concentration corresponding to the mid-point of each of the acid base transition

samples, then the color change was judged by naked eyes. For example, a sample that gave a red coloration with better yellow, but was yellow with a small amount of red, was estimated to have acid strength, $H_0 = 3.3 \sim 2.0$ or rank III. For comparison, acid strength was also measured

Table 4 Ordinary numbers to express H_0 values

Rank	H_0
I	+5.0 ~ +4.0
II	+4.0 ~ +3.3
III	+3.3 ~ +2.0
IV	+2.0 ~ -1.5
V	-1.5 ~ -3.0
VI	-3.0 ~ -5.6

samples, then the color change was judged by naked eyes. For example, a sample that gave a red coloration with butter yellow, but was yellow with o-aminoazotoluene, was estimated to have acid strength, $H_0 = 3.3 \sim 2$ or rank III. For comparison, acid strength was also measured for the mixture of alumina with NaH_2PO_4 and/or H_3PO_4 , that was equilibrated under various RH sets with the same manner.

The some heated samples were subjected for measurement with infrared spectroscopy, to observe possible change in the structure of allophane.

4-3 Results and discussion

4-3-1 Samples with Sodium Saturation

Table 5 gives measured acid strength of the allophane samples before and after the P adsorption, for the sodium saturated sample (Na-type). Generally the acid strength of sample with high Si/Al ratio (KnP) is stronger than that of the low ratio ones (KyP), under RH of 31% and after heating at 100 °C. This result agrees well with investigation reported before (Henmi and Wada, 1974; Henmi et al, 1997). Here, KnP has greater ratio

Table 5 Measured acid strength (H_0) of the sample before and after the P adsorption (Na-type)

Sample	RH (%)			after heating at 105°C
	100	76	31	
KyP (without P)	I	II	II	III
P=142mmolkg ⁻¹ (*)	II	III	III	V
P=190mmolkg ⁻¹	II	III	III	V
P=304mmolkg ⁻¹	II	III	III	V
P=399mmolkg ⁻¹	II	III	IV	V
P=420mmolkg ⁻¹	II	III	IV	V
KnP (without P)	I	II	II	IV
P=130mmolkg ⁻¹	II	III	IV	V
P=200mmolkg ⁻¹	II	III	V	V
P=275mmolkg ⁻¹	II	III	V	V
P=302mmolkg ⁻¹	II	III	V	V
Al ₂ O ₃	I	I	I	I
Al ₂ O ₃ + NaH ₂ PO ₄ ⁽¹⁾	II	II	II	II
Al ₂ O ₃ + NaH ₂ PO ₄ ⁽²⁾	II	II	II	II

(*) The above data indicated amount of P adsorbed

(1) and (2) indicated mixture of Al₂O₃ with NaH₂PO₄ of 300 and 420 mmol kg⁻¹, respectively

of Si/Al than the KyP has, so the KnP sample can be assumed as SiO_4 tetrahedra adsorption product of KyP. The stronger acidity of the KnP sample may be due to enhancement in Brønsted acidity on silanol group, caused by the adsorption of SiO_4 tetrahedra on its structure, as reported by Henmi et al. (1997).

For all cases, the acid strength of both allophane samples increased with decreasing RH. This means that the acid strength of the samples was strongly affected by water adsorbed on mineral surfaces, RH. These results agree well with the observations reported before, either for allophane or for other clay minerals (Mortland and Raman, 1968; Frenkel, 1974; Henmi and Wada, 1974, Wu et al., 1992). At RH of 100%, the acid strength of KyP and KnP was the lowest ones and was same each other, with rank of I. This may be because at that condition, water molecules occupied a large parts of the clay surfaces, with the result only weakly Brønsted acid developing on their surface.

Both samples showed increase in the acid strength after the P adsorption, under all of the RH sets observed. However, degree of increment was not so different each

other, among various amounts of P adsorbed. In case of KyP, the degree of increment was same among various amount of P adsorbed, until the P adsorbed of 304 mmol kg⁻¹. The acid strength increased from rank I into rank II under RH of 100% and from rank II to III under RHs of 76 and 31%. However, at the range of P adsorbed of 399 mmol kg⁻¹ and more, the degree of strengthening is greater at the RH of 31%, with the acid strength increased from rank II to IV. The strongest acidity was found at RH~0% (after heating at 105 °C). The H₀ value was fall into rank V, which was same for the all-various amounts of P adsorbed, for both KyP and KnP samples. The same degree of strengthening may be because the samples loss almost all of water adsorbed on the surface of allophane, so as the acid strength is only determined by exchangeable Na (Si-ONa or P-ONa) and hydroxyl on the silanol (Si-OH) and aluminol (Al-OH₂⁺) groups.

For KnP with P adsorption of 130 mmol kg⁻¹ the acid strength increased from rank I to II, from II to III, from II to IV, and from IV to V, under RHs of 100, 76, 31, and ~0%, respectively. Furthermore, the degree of strengthening was greater at the higher region, at the

range P adsorption of 200 mmol kg^{-1} and more, but only at the RH of 31%, and no variation with the H_0 values with increasing amount of P adsorbed. The H_0 increased from rank III to V, as strong as with that was observed at RH~0%.

Furthermore, the acid strength of alumina powder increased from rank I to II, after mixed with NaH_2PO_4 , at RH~0% (after heating at 100°C). However, washing treatment to the mixture of alumina with NaH_2PO_4 caused decrease in its surface acidity. This means only "physical adsorption" occurred in alumina, leading to the implication that the acidity (rank II) is the acidity of NaH_2PO_4 itself. As shown at the table 5, the acidity of the P adsorption complexes (samples that are adsorbed P) are stronger than that of the mixture of alumina powder with NaH_2PO_4 , for all cases, indicating that the acidity of phosphated sample is stronger than the acidity of phosphate (NaH_2PO_4) itself.

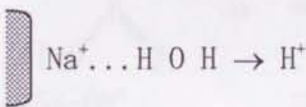
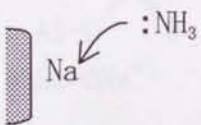
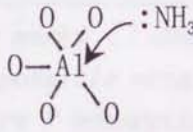
As described in the introduction, the surface of soils or clay minerals are known to have two kinds of acidity, namely Brønsted acidity and Lewis Acidity. Brønsted acid origins from protons (H^+) on permanent

negative charge, water molecules coordinated to exchangeable cations, and hydroxyl groups at crystal edges or functional groups, while Lewis acid arises from coordination unsaturated structural Al or Si and from exchangeable cations (Wu et al., 1992).

In this experimental data (Table 5) probably the acidity of samples origins from water molecules coordinated to exchangeable Na^+ (at higher RH), hydroxyl groups from silanol and aluminol on the allophane structure, and from exchangeable Na^+ (at lower RH). The two former are Brønsted acidity, and the last one is Lewis acidity. Origin of acidity of allophane could be schemed, as shown at table 6a and 6b.

In this experimental condition, the strong Lewis acidity due to coordination unsaturated structural Al or Si may not exist. That acidity arises when allophane loss some hydroxyl groups. The reason for absence of above strong acidity is that the samples were only heated up to 105 °C, whereas dehydroxylation of allophane occurs at temperature of 300 °C or more (Henmi and Wada, 1974). Observation by infrared spectroscopy

Table 6a Possible origin of surface acidity of allophane samples,
before P adsorption

Source of acidity	Acidity type	Relatively acid strength
1 Functional groups		
$\text{Si-OH} \rightarrow \text{Si-O}^- + \text{H}^+$	Brønsted	Medium~strong
$\text{Al-OH}_2^+ \rightarrow \text{Al-OH} + \text{H}^+$	Brønsted	Medium~strong
2 Water on exchangeable Sodium at Si-ONa or Al-ONa	Brønsted	Weak
		
3 Exchangeable sodium (Si-ONa or Al-ONa)	Lewis	Medium~strong
		
4 Coordination unsaturated Aluminum/silicon	Lewis	Very strong
		

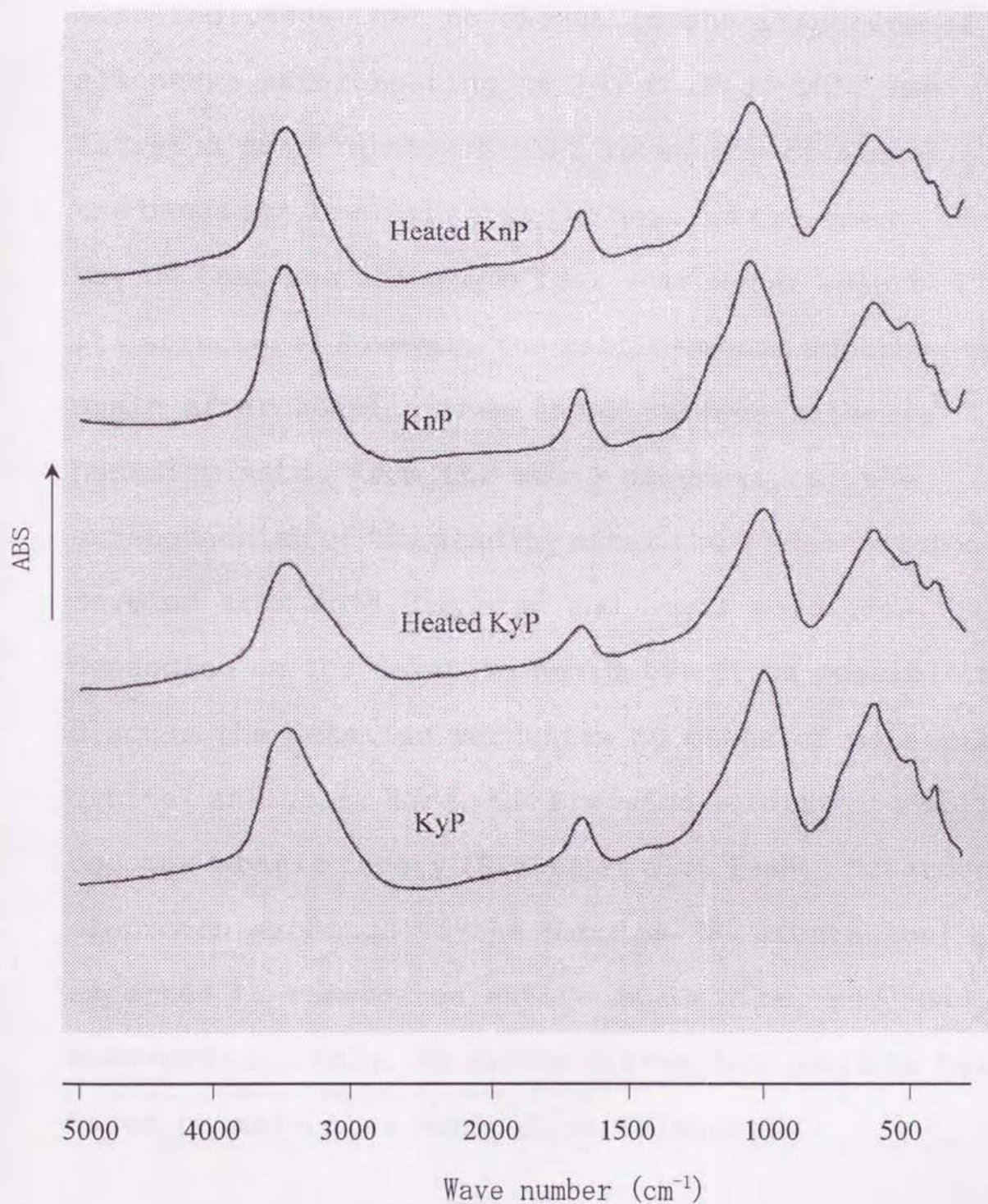


Fig. 15 Diffuse reflectance IR spectra of the allophane samples before and after heating treatment at 105°C

also indicates that no change in the structure of allophane after heating at 105 °C (Fig. 15). The infrared spectra showed that intensity of almost all the bands are lowered after the heating treatment. This may be that the allophane lost some water adsorbed on its structure. However, the samples would adsorb water again after keeping them under various relative humidity sets. From the above discussions, the strengthening of the acidity after the P adsorption may develop from both Brønsted and Lewis acidities, depending on the relative humidity. It is possible to discuss the detailed mechanism by means of molecular orbital analysis. Here, the Brønsted acidity of a solid becomes a basic theory (Siegel et al., 1988). Treatment of proton exchange to the samples (H^+ saturation) is expected to remove the entire Lewis site, and remain Brønsted site only, so as the discussion could be held based on molecular orbital calculation.

4-3-2 Samples with H Saturation

Table 7 shows measured acid strength of the samples after the adsorption followed by H^+ saturation.

Table 7 Measured acid strength of the allophane samples after P adsorption followed by H⁺ saturation

Sample	RH (%)			After heating at 100°C
	100	76	31	
H-KyP	I	II	III	V
P=190 mmol kg ⁻¹	II	III	IV	V
P=304 mmol kg ⁻¹	II	III	IV	V
P=399 mmol kg ⁻¹	II	III	V	V
P=420 mmol kg ⁻¹	II	III	V	V
H-KnP	II	III	V	V
P=130 mmol kg ⁻¹	II	III	V	V
P=200 mmol kg ⁻¹	II	III	V	V
P=275 mmol kg ⁻¹	III	V	VI	VI
P=302 mmol kg ⁻¹	III	V	VI	VI
P=365 mmol kg ⁻¹	III	V	VI	VI
Al ₂ O ₃	I	I	I	II
Al ₂ O ₃ + H ₃ PO ₄ ⁽¹⁾	II	II	II	III
Al ₂ O ₃ + H ₃ PO ₄ ⁽²⁾	II	II	II	III

(*) The above data indicated amount of P adsorbed

⁽¹⁾ and ⁽²⁾ indicated mixture of Al₂O₃ with H₃PO₄ of 300 and 420 mmol kg⁻¹, respectively

For both samples the acid strength increased with H^+ saturation treatment, especially at lower RH sets. The acid strength of H^+ saturated KnP samples are stronger than that of KyP samples, except that under $RH \sim 0\%$, the acid strength was same each other. Possible origins of acidity of the original samples are water adsorbed on the allophane surface, and hydroxyl of the silanol groups.

The acid strength is tend to be stronger for the samples after the P adsorption, compared with that for original samples with H^+ saturation, observed for the both samples. The acid strength of KyP sample increased from rank I to rank II, from rank II to III, and from III to IV, under RHs of 100, 76, and 31%, respectively, over the range of P adsorption up to 304 mmol kg^{-1} . However, the acid strength did not increase, and still kept at rank V for the heated sample ($RH \sim 0\%$), over the entire range amount of the P adsorption. At higher P adsorption (399 mmol kg^{-1} and more) the degree of increment was greater under RH of 31%. The H_0 increased from rank III to V, as strong as that under $RH \sim 0\%$.

In case of KnP sample, the acid strength did not

increase at the low P adsorption range (130 and 200 mmol kg⁻¹), for the all of RHs observed. At range P adsorption of 275 mmol kg⁻¹ and more, the acid strength increased, under all of RH sets. The degree of increment was same each other, over range of various amount of P adsorbed (275 mmol kg⁻¹ and more). The acid strength, H₀ values increased from rank II to III, and from III to V, under the RHs of 100 and 76%, respectively. At the lower RHs (31% and after heating at 100 °C), the acid strength increased from rank V to rank VI.

Furthermore, the acid strength was also stronger for allophane samples after the P adsorption and followed by H⁺ saturation than the acid strength of the mixture of alumina powder with H₃PO₄. However washing treatment to those mixtures decreased their acidity. This means that the H₃PO₄ was only adsorbed physically on the alumina powder, leading to conclusion that the acid strength of the phosphate adsorption complexes was stronger than that of phosphoric acid itself.

In those cases, the acidity probably develop from water adsorbed on surface of allophane and from hydroxyl groups (Si-OH, P-OH, or Al-OH₂⁺), for all of

the samples, because they were saturated with proton. Both types are Brønsted acidity, therefore the discussion could be proceeded to the molecular orbital analysis. As mentioned above, the analysis is only suitable for the Brønsted acidity.

Two possibilities are proposed for mechanism of the strengthening in the acidity caused by the P adsorption on allophane. First, the enhancement in the acidity came from the P-OH groups, newly formed on allophane after the P adsorption. Second, the enhancement is due to increase in dissociation of proton from the silanol groups on the structure of allophane, due to the P adsorption. Molecular orbital calculation was carried out to elucidate which is the mechanism occurred.

4-3-3 Analysis by Molecular Orbital Method

The acidity of a molecule can be estimated from the difference between energy of anion and that of neutral molecule (Siggel and Thomas, 1986), expressed as follow:

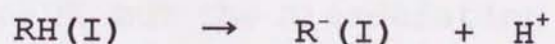
$$A = E_a - E_m \quad (5)$$

where A is acidity of a molecule in gas phase, E_a is the total energy of anion, and E_m is total energy of neutral molecule. Based on that theory, the anion and molecule could be represented by dissociated and undissociated forms, respectively for the Brønsted acidity of a molecule.

Generally, Brønsted acidity is estimated by pKa value or ΔG (free energy change) of reaction (Siggel et al., 1988). The ΔG can be approximated by delta H (ΔH), the difference in heat of formation (H) between the products and reactants ($\Delta H = H_{\text{products}} - H_{\text{reactants}}$). The dissociation reaction is expressed as follow:



The principle of calculation is, when comparing reactions of two similar compounds, RH (I) and RH (II), we only need to calculate H of dissociated and undissociate forms.



Lower ΔH of a reaction indicates stronger in the Brønsted acidity.

The calculation was done with MOPAC program, with semi-empirical MNDO-PM3 basis set (Stewart, 1989) which is incorporated in CAChe system for Windows (CAChe Scientific Inc., Sony Tektronix Corporation). The basis set provides closest results with the experimental condition.

For the molecular orbital calculation, cluster models for allophane were built up with Al normal octahedra and Si tetrahedra by using bond distances of Al-O = 0.1912 nm, Si-O = 0.1618 nm and O-H = 0.0944 nm. Figure 16 gives model clusters for the calculation. The clusters consisted of six Al atoms, one Si atoms, and several O and H atoms. Model A simulates model cluster of the original allophane. Model B simulates allophane with phosphate adsorbed on its structure (phosphate adsorption complex). On the model B, two-H atoms bonded to the Al (Al-OH) were removed and were replaced with one phosphate anion (H_2PO_4^-). Model C is similar to the model B, but the dissociation sites are different each other. Model D describes phosphoric acid.

Protons numbered from 1 to 4 simulate proton to dissociate. Proton No. 1 represents proton of the

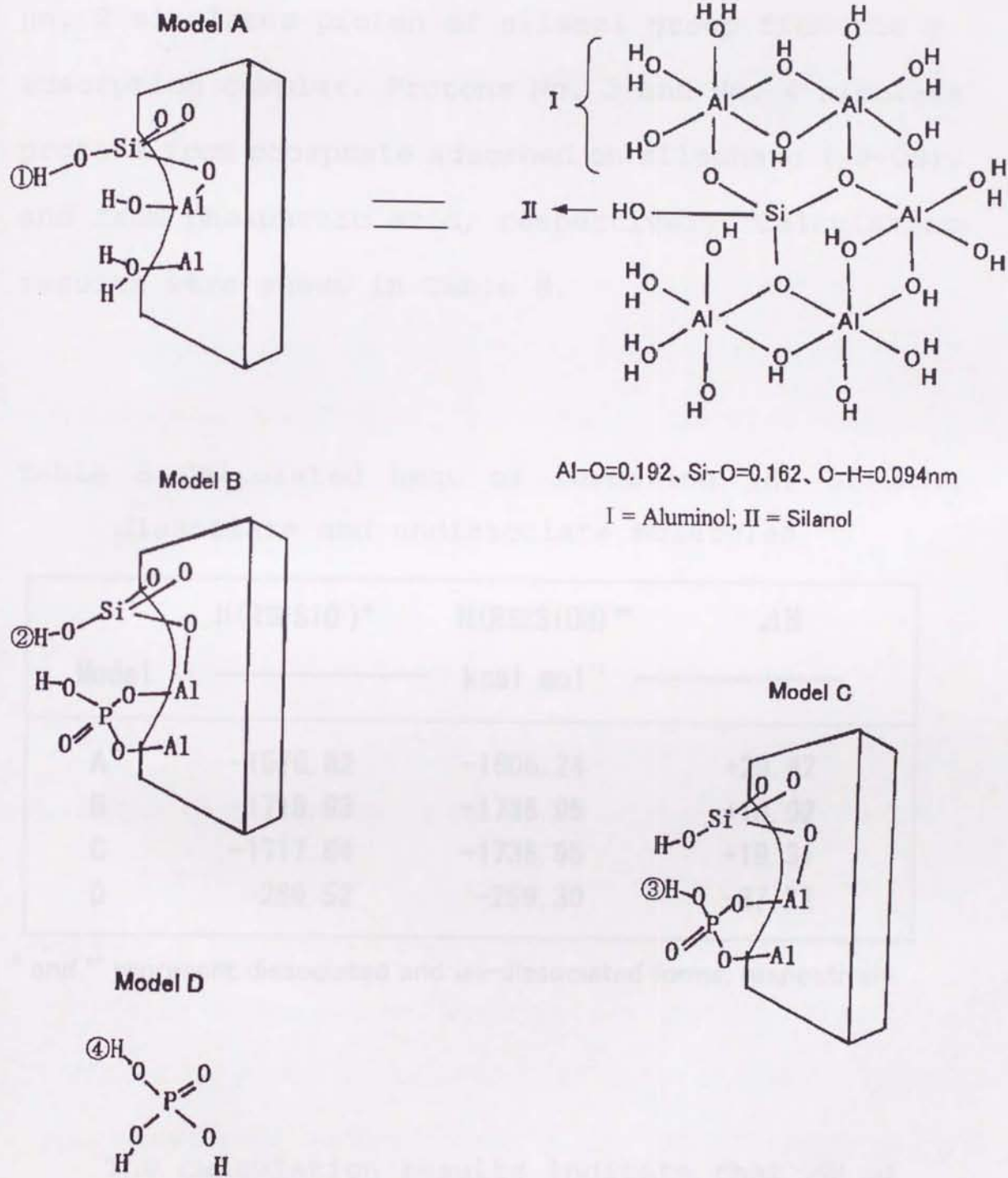


Fig. 16 Cluster models of allophane used for molecular orbital calculation for the surface acidity

Silanol group of from the original allophane. Proton no. 2 simulates proton of silanol group from the P adsorption complex. Protons No. 3 and No. 4 simulate protons from phosphate adsorbed on allophane (-P-OH), and from phosphoric acid, respectively. Calculation results were shown in Table 8.

Table 8 Calculated heat of formation (H) of some dissociate and undissociate molecules

Model	H(R≡SiO)*	H(R≡SiOH)**	ΔH
	—————	kcal mol ⁻¹	—————
A	-1576.82	-1606.24	+29.42
B	-1718.93	-1736.95	+18.02
C	-1717.64	-1736.95	+19.31
D	-286.52	-259.30	-27.22

* and ** represent dissociated and un-dissociated forms, respectively

The calculation results indicate that ΔH of dissociation of proton No. 2 is lower than that of proton No. 1. This means that Brønsted acidity of silanol groups of the P adsorption complex is greater than that

of original allophane. This may be because phosphate adsorbed cause enhancement Brønsted acidity of the silanol groups in the structure of allophane.

Furthermore, the ΔH of dissociation proton No. 3 is smaller than that of proton No. 4. This means that the acidity of phosphoric acid is lowered after adsorption on the structure of allophane. From the above calculation results it is concluded that the strengthening in acidity is not due to dissociation of phosphate adsorbed on allophane (P-OH), but due to dissociation of silanol group, caused by enhancement its Brønsted acidity after the P adsorption.

Henmi et al. (1997) found enhancement in acid strength of allophane by orthosilicic acid adsorption. They suggested that the enhancement of Brønsted acidity of silanol groups occurred due to interaction between O-H of the newly formed silanol group with nearby O-H of silanol groups, with the result the nearby silanol group underwent enhancement in the Brønsted acidity, then deprotonation occurred. Based on the above finding, the interaction may also occur between P-OH group and Si-OH group to accelerate dissociation of proton from

silanol group (de-protonation). The possible interaction is shown in Fig. 17. Model E describes interaction between P-OH and Si-OH attached to the gibbsite sheet (monomeric SiO_4 tetrahedra). Model F describes interaction between P-OH and weakly bonded Si-OH (polymeric SiO_4 tetrahedra). On the model E, proton No. 5 is located close to oxygen atom No. 7, so they interact each other, with the result proton No. 8 (with triangle mark) is released (deprotonation). Similar explanation holds for the model F. Interaction may occur between proton No. 5 and oxygen atom No. 9, with the result proton No. 10 is released.

The dissociation of silanol group due to P adsorption not only increase the acid strength, but also provide new negative charge for cation exchange capacity (CEC) sites on the surface of allophane, because the main negative sites of allophane is the silanol groups. The increase in the negative charge caused by P adsorption was also observed in this study, and will be described in the next chapter.

4-4 Conclusions

1 Phosphate adsorption on the surface of aluminosilicates

2 The enhanced adsorption of phosphate on the surface of aluminosilicates is due to the formation of inner-sphere complexes. The interaction between Si-OH and P-OH groups is shown in the following scheme.

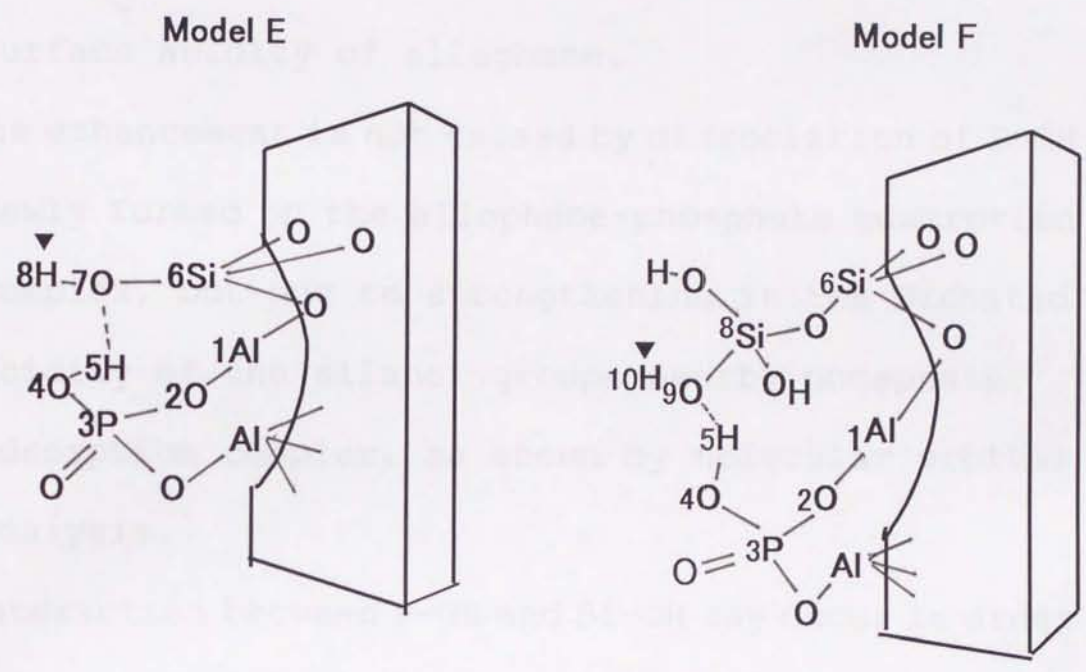


Fig. 17 Scheme of interaction between Si-OH and P-OH

4-4 Conclusions

- 1 Phosphate adsorption causes enhancement in the surface acidity of allophane.
- 2 The enhancement is not caused by dissociation of P-OH newly formed on the allophane-phosphate adsorption complex, but due to strengthening in the Brønsted acidity of the silanol groups nearby phosphate adsorption complex, as shown by molecular orbital analysis.
- 3 Interaction between P-OH and Si-OH may occur in order to accelerate dissociation of proton release from silanol groups.
- 4 The increase in the Brønsted acidity of Si-OH groups induced by the P adsorption will also increase negative charge for cation exchange capacity (CEC) sites of allophane.

Chapter 5 CHANGE IN SURFACE CHARGE WITH P ADSORPTION ON ALLOPHANE

5-1 Introduction

There have been many studies showing increase in negative charge and/or decrease in positive charge of soils and clay minerals after phosphate application (Schalscha et al., 1974; Sawhney, 1974; Rajan, 1976; Naidu et al., 1990). The simplest explanation for this phenomenon is that the negative charge of the phosphate anion (H_2PO_4^- or HPO_4^{2-}) was added to the soil materials and clay minerals through adsorption. The negative charge addition is remarkable for such as Fe- and Al-hydroxyoxides, volcanic ash soils, or allophanic clays, because they have large capacities for phosphate adsorption (Mekaru and Uehara, 1972; Nanzyo, 1988; Matar et al., 1992).

During the phosphate adsorption, increases in solution pH were also observed under conditions where all or part of the phosphate existed as anion species (Rajan, 1976; Gunjigake and Wada, 1981; Nanzyo, 1995). The increase in pH is due to condensation reaction

between Al(Fe)-OH groups of clays and P-O⁻ groups of the phosphate anion, which results in formation of Al(Fe)-O-P bonding and release of OH⁻ to solution phase. From charge balance requirement, the amount of negative charge brought by the adsorbed phosphate should be equal to the sum of observed negative charge increase, positive charge decrease, and final OH⁻ released.

The observed change in surface charges, however, includes the effect of increase in solution pH, because surface charges of most soils and clay minerals are variable in nature. For example, addition of NaOH solution to a soil or clay suspension will result in increase in negative charge, decrease in positive charge, and increase in suspension pH. In this case, variable charge characteristics of the soil or clay remains unchanged, and negative (positive) charge values after the NaOH addition will locate just on the pH vs. negative (positive) charge curves of the original sample. The addition of NaOH increased negative charge and decreased positive charge, but the charge characteristics of the sample did not change.

Therefore, in estimating the effect of phosphate

adsorption on the charge characteristics of soils and clay minerals, change in the amounts of surface charges due to pH increase after the adsorption, must be taken into account. In this study, we determined net effect of phosphate adsorption on the charge characteristics of allophane by comparing pH vs. charge curves between original and phosphated allophane samples under a same solution pH.

Allophane was selected as phosphate adsorbent because it has high capacity for phosphate adsorption and is one of the major components in clay of volcanic ash soils such as Andepts. As mentioned above, Allophane is composed of gibbsite sheet with SiO_4 tetrahedra attached to it (Fig. 1), and has hollow spherical morphology locating the SiO_4 tetrahedra inside of the sphere (Parfitt and Henmi, 1980). Wall of the hollow sphere, nano-ball, has some holes (defects) resulting in Al-OH and Al-OH₂ groups exposed (Paterson, 1977; Wada and Wada, 1977). The main phosphate adsorption site and variable positive charge site are the aluminol groups. The variable negative charge site is silanol (Si-OH) group of the SiO_4

tetrahedra (Harada and Wada, 1973; Wada, 1989), and some of the SiO_4 tetrahedra act as phosphate adsorption site (Johan et al., 1997).

An assumption was taken that, with phosphate adsorption, the allophane was converted to new compound, allophane-phosphate adsorption complex. Under the assumption, discussion was held on the reason for the difference in charge characteristics between allophane and the complex, together with phosphate adsorption mechanism, using the detailed chemical structure of nano-ball allophane.

5-2 Materials and Methods

The allophane samples ($<0.2\ \mu\text{m}$) described above (KyP and KnP) were used for the experiment. The sample suspensions were previously equilibrated in 10 mM NaCl. Phosphate adsorption experiments and determination of positive and negative charges of the allophane samples were carried out in NaCl background solution. For phosphate adsorption experiment, 25 mL of up to 4 mM NaH_2PO_4 solution was added to 5 mL of sample suspension containing 50 mg of allophane, in a 50 mL polypropylene

centrifuge tube of known weight, and shaken for 24 h. Total Na concentration of the NaH_2PO_4 solutions were adjusted at 10 mM by adding NaCl. The phosphate adsorption experiments were carried out at different initial pHs: pH values of the allophane suspension and NaH_2PO_4 solution were adjusted at a same value before mixing by adding HCl or NaOH solution. After shaking for 24 h, the suspension was centrifuged and the supernatant was analyzed for P by ascorbic acid method (Murphy and Riley, 1962), for Na by atomic adsorption spectrophotometry, for Cl by mercury (II) thiocyanate method (Huang and Johns, 1966), and for pH with pH meter. The equilibrium pH of the blank run (P concentration is 0) was considered as the initial pH before phosphate adsorption for each series. Part of the supernatant was titrated with HCl solution from final to initial pH to determine the amount of final OH^- release. After decanting the supernatant, weight of the centrifuge tube plus residue was measured to know the volume of entrained solution. The residue was washed with 30 ml of 1 M NH_4NO_3 three times and the amounts of extracted Na and Cl were measured. The amounts of both negative

and positive charges of sample were determined from the amounts of Na^+ and Cl^- retained at equilibrium: extracted Na or Cl with 1 M NH_4NO_3 minus those in the entrained solution.

5-3 Results and Discussion

5-3-1 Net Effect of Phosphate Adsorption on Charges

Charge characteristics of original samples in 10 mM NaCl are shown as circle symbols and solid lines in Fig. 18a and 18b for KyP and KnP, respectively, in which the amounts of negative and positive charges, Na^+ and Cl^- retained, are plotted against equilibrium pH. Under such condition, it is known that the amounts of both Na^+ and Cl^- retained are determined by equilibrium pH (Wada, 1983). Each series of experimental points in Fig. 18 fitted to a curve, indicating unequivocal relationship between the amounts of negative and positive charges and equilibrium pH. With increasing equilibrium pH, the amount of negative charge increases, whereas that of positive charge decreases for both the samples. Under pHs of about between 4 and 7, the two allophane samples have both negative and positive

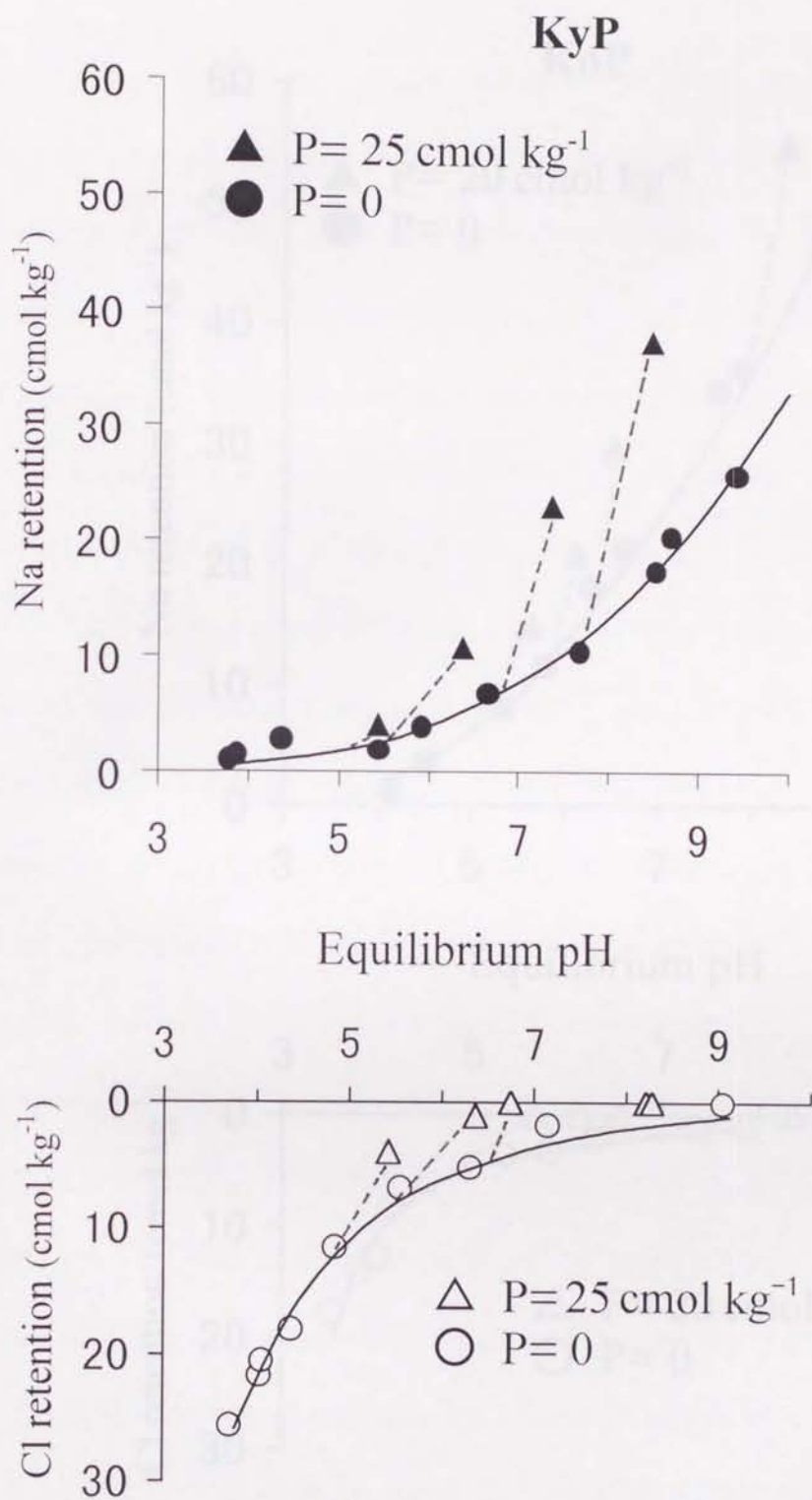


Fig. 18a Charge Characteristics of KyP samples in 10 mM NaCl, with 0 and 25 cmol kg⁻¹ P adsorption

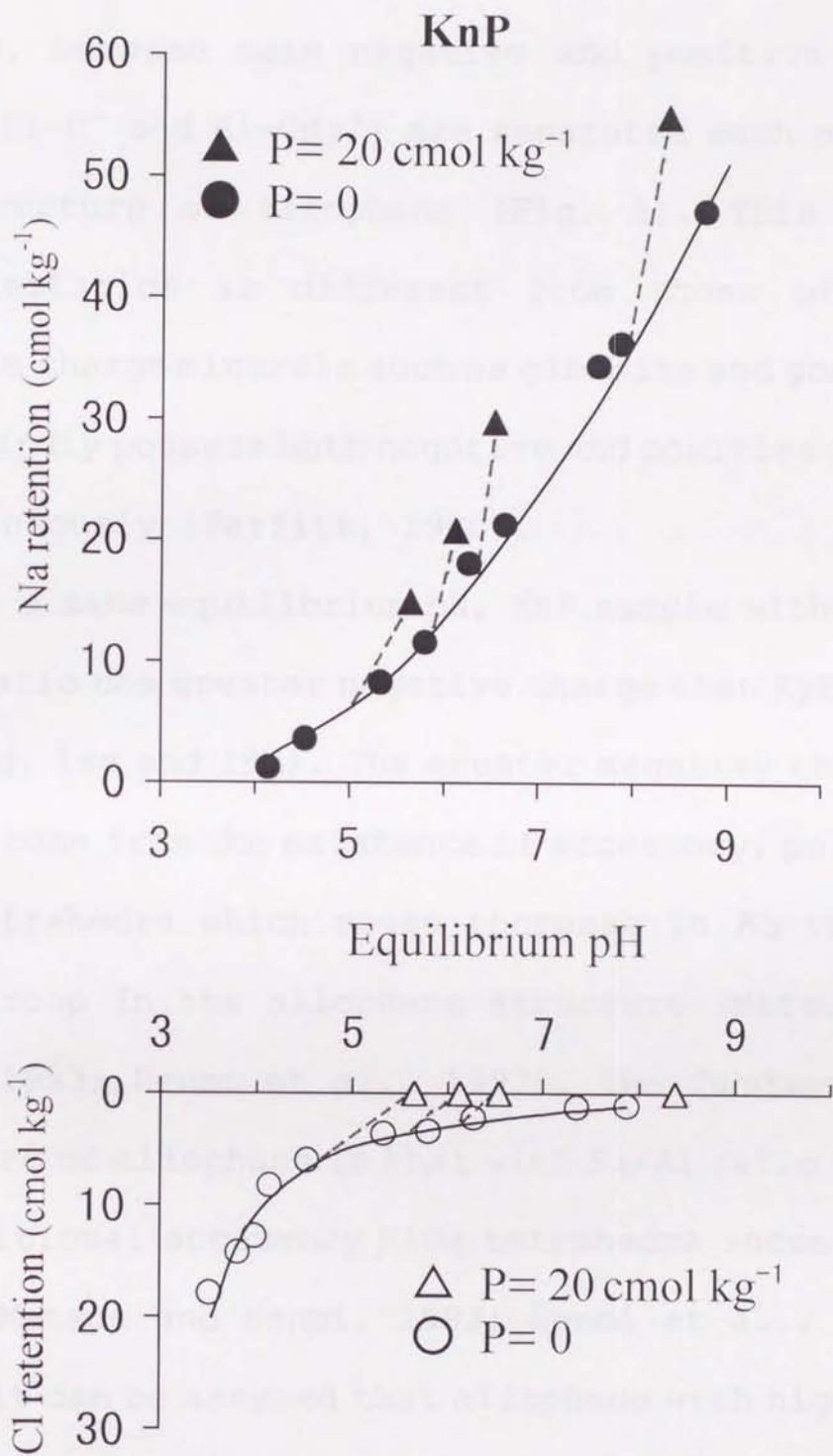


Fig. 18b Charge characteristics of KnP samples in 10 mM NaCl, with 0 and 20 cmol kg⁻¹ P adsorption

charges, because main negative and positive charge sites (Si-O^- and Al-OH_2^+) are separated each other in the structure of allophane (Fig. 1). This charge characteristics is different from those of other variable charge minerals such as gibbsite and goethite, which hardly possess both negative and positive charges simultaneously (Parfitt, 1980).

At a same equilibrium pH, KnP sample with higher Si/Al ratio has greater negative charge than KyP sample has (Fig. 18a and 18b). The greater negative charge of the KnP come from the existence of accessory, polymeric SiO_4 tetrahedra which cause increase in K_a value of Si-OH group in the allophane structure (Matsue and Henmi, 1993; Henmi et al., 1997). The fundamental structure of allophane is that with Si/Al ratio of 0.5, and additional accessory SiO_4 tetrahedra increase the ratio (Matsue and Henmi, 1993; Henmi et al., 1997). Hence, it can be assumed that allophane with high Si/Al ratio, such as KnP sample, is a SiO_4 tetrahedron adsorption product of allophane with low Si/Al ratio, such as the KyP sample, and that the adsorbed SiO_4 tetrahedra caused an increase in the amount of negative

charge. Lower positive charge of KnP than KyP at a same equilibrium pH is mainly due to its lower aluminol groups content per unit mass: the amount of aluminol groups per unit mass decreases with increasing Si/Al ratio of allophane (Son et al., 1998). Steric hindrance effect by the polymeric SiO₄ tetrahedra on the aluminol groups at the pore region may partly account for the lower positive charge of the KnP sample.

Charge characteristics of the two allophane samples after the phosphate adsorption are shown in Fig. 18a and 18b as triangle symbols. The phosphated KyP and KnP samples retained 25 and 20 cmol kg⁻¹ of P, respectively, over the pH range examined. The concentration of added NaH₂PO₄ solution was adjusted so as to give desired phosphate retention value at equilibrium. Since maximum phosphate adsorption of the samples at about pH 6 in 10 mM NaCl were 55 and 45 cmol kg⁻¹ for KyP and KnP samples, respectively (Johan et al., 1997), the phosphate retention value for KnP was adjusted smaller than that for KyP sample. Broken lines in Fig. 18a and 18b indicate changes in the amounts of charges and solution pH with the adsorption. In all

cases, pH of the supernatant solution increased with the phosphate adsorption, indicating OH^- release with the adsorption.

Figs. 18a and 18b show that, with the phosphate adsorption, both the negative and positive charge characteristics changed from those of the each original samples: negative charge increased, and positive charge decreased. Because the solution pH increased with the adsorption, observed changes in negative and positive charges, difference in charges of allophane before and after the phosphate adsorption, are not the net change due to the adsorbed phosphate. Figure 19 shows schematic relationships among the observed change, the change due to pH increase and the net change in surface negative and positive charges. The net effect of the phosphate adsorption on the amount of negative charge was positive, and that on positive charge was negative. Adsorption of a negatively charged substance does not necessarily increase the negative charge for an adsorbent. In case of $\text{B}(\text{OH})_4^-$ adsorption on the KyP sample, negative charge value of $\text{B}(\text{OH})_4^-$ adsorbed sample located below the curve of the original

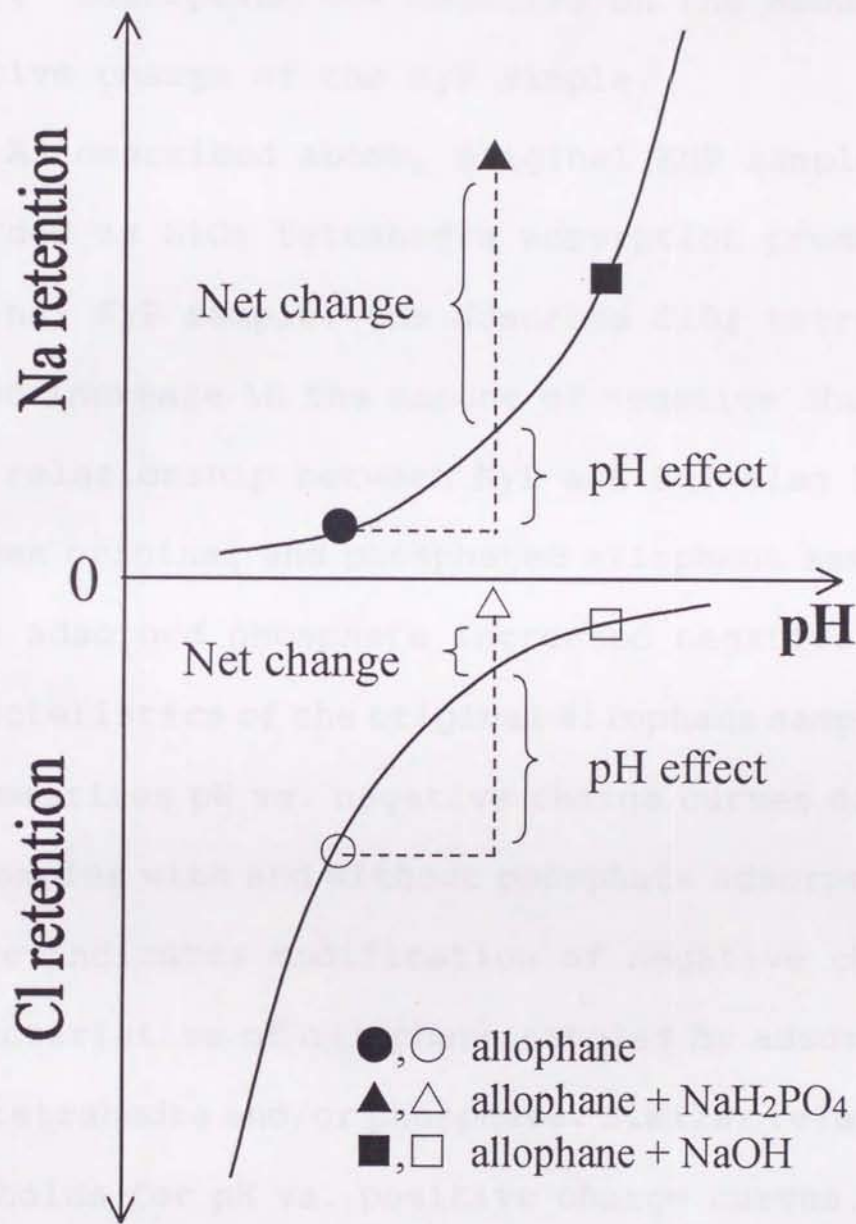


Fig. 19 Schematic relationship among observed change, change due to pH effect and net change in surface negative and positive charges

sample in the plot same as Fig. 19 (will be published elsewhere). This indicates that net effect of the $B(OH)_4^-$ adsorption was negative on the amount of negative charge of the KyP sample.

As described above, original KnP sample can be regarded as SiO_4 tetrahedra adsorption product of original KyP sample: the adsorbed SiO_4 tetrahedra caused increase in the amount of negative charge. The same relationship between KyP and KnP also holds between original and phosphated allophane samples, in which adsorbed phosphate increased negative charge characteristics of the original allophane samples. Fig. 20 summarizes pH vs. negative charge curves of KyP and KnP samples with and without phosphate adsorption. The figure indicates modification of negative charge characteristics of allophane samples by adsorption of SiO_4 tetrahedra and/or phosphate. Similar relationship also holds for pH vs. positive charge curves. Fig. 20 also indicates that imogolite (KiG), tubular morphology with the same chemical composition and local structure as the fundamental allophane ($Si/Al=0.5$), has less negative charge than the KyP sample with $Si/Al=0.67$.

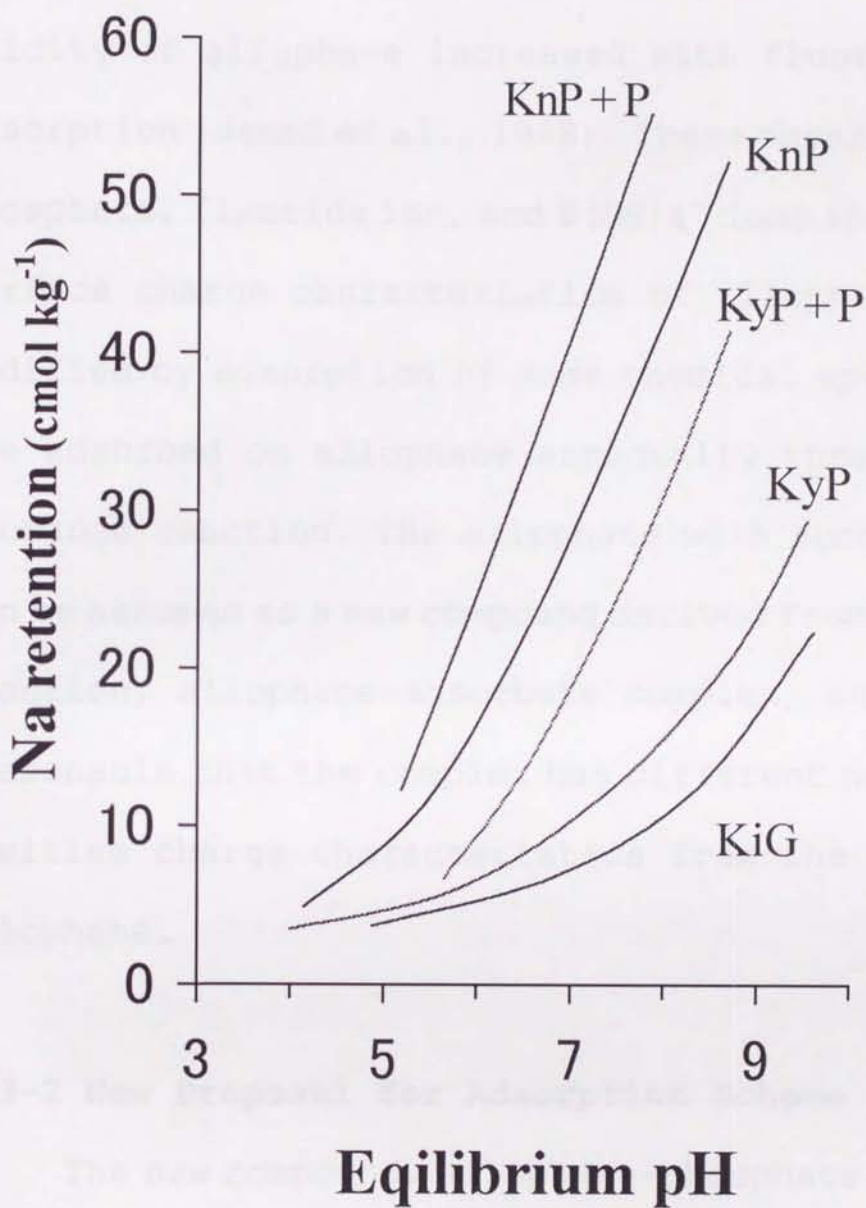


Fig. 20 Summary of pH vs. negative charge curves of KyP and KnP samples with and without P adsorption. KiG: imogolite sample with Si/Al=0.5

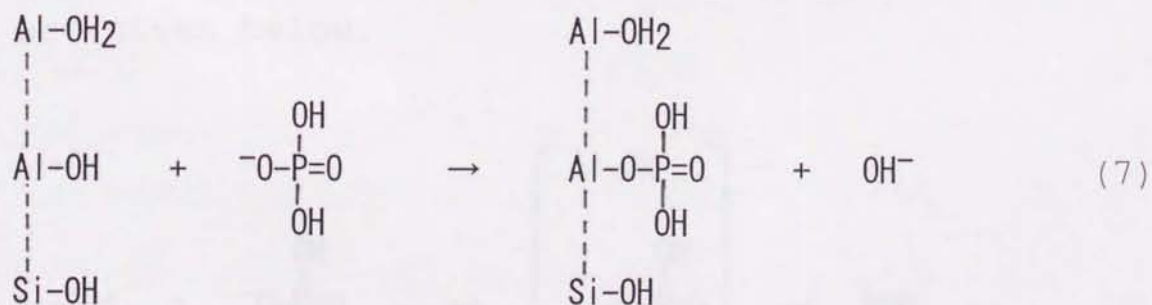
Other study also found that negative charge and surface acidity of allophane increased with fluoride ion adsorption (Henmi et al., 1998). These observations for phosphate, fluoride ion, and $B(OH)_4^-$ ions indicate that surface charge characteristics of allophane can be modified by adsorption of some chemical species which are adsorbed on allophane especially through ligand exchange reaction. The allophane with such adsorbate can be assumed as a new compound derived from adsorption reaction, allophane-adsorbate complex, and it is reasonable that the complex has different negative and positive charge characteristics from the original allophane.

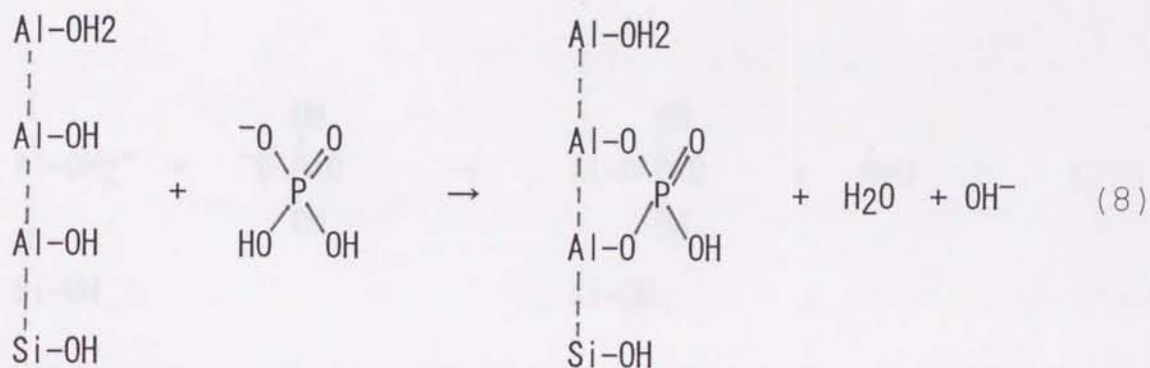
5-3-2 New Proposal for Adsorption Scheme

The new compound, allophane-phosphate adsorption complex, had higher negative and lower positive charges compared to original allophane. The explanation of the difference in surface charge characteristics between the two is as follow, in relation with new adsorption scheme and detailed chemical structure of allophane (Fig. 1). At first, it is assumed that one OH^- is

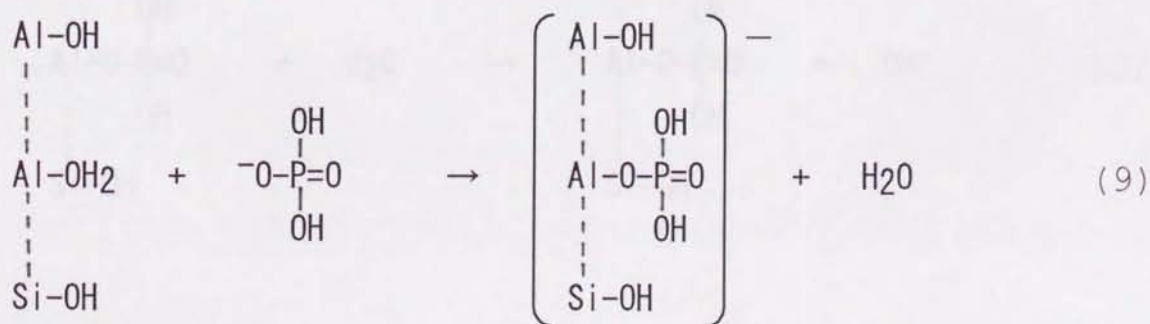
initially released with adsorption of one H_2PO_4^- anion. The assumption is valid, and the reasons for the validity are given below.

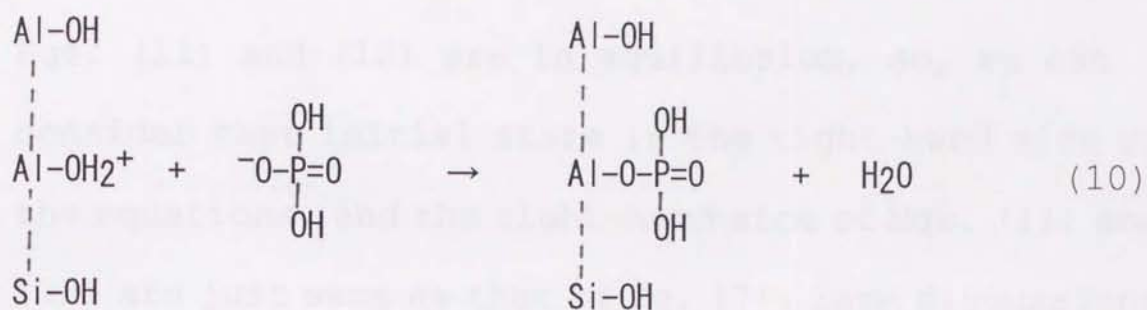
Possible adsorption sites for the H_2PO_4^- anion are Al-OH and Al-OH₂ groups located at the pore region of allophane (Fig. 1), and adsorption on Al-OH₂⁺ group also occur under lower pH region. Allophane samples contain more than 200 cmol kg⁻¹ of these aluminol groups, and the amount is much greater than that of the adsorbed phosphate. Among the aluminol groups, it is supposed that the H_2PO_4^- anion reacts only with Al-OH group. Reaction formulae for mononuclear and binuclear bondings are written as follows by ignoring Na⁺ and Cl⁻ for simplification.



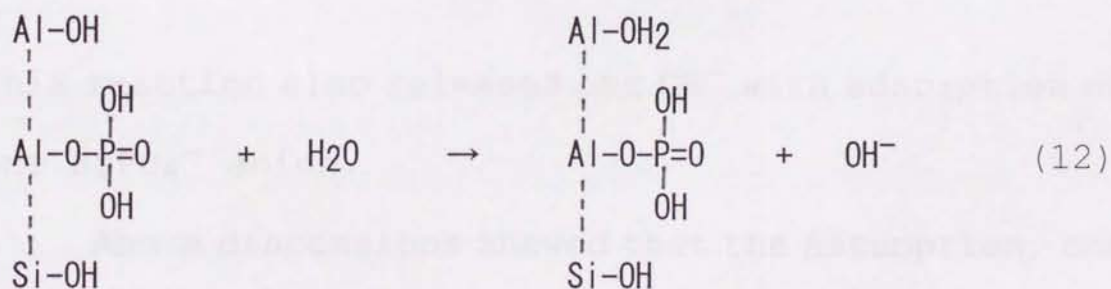
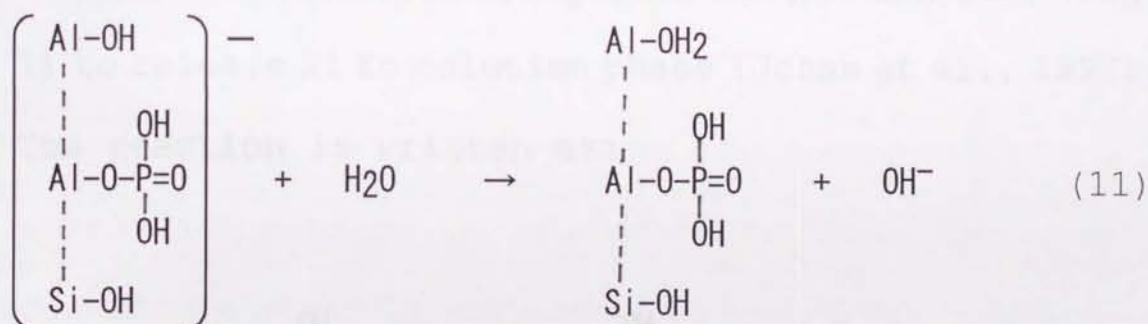


In the equations, the top Al-OH₂ and the bottom Si-OH represent those near phosphate adsorption site. Eqs. (7) and (8) indicate that one OH⁻ is released with one H₂PO₄⁻ adsorption. On adsorption of one HPO₄²⁻ anion at higher pH region, two OH⁻ are released. The supposition that phosphate anion reacts only with Al-OH group is not realistic, since Al-OH₂ and Al-OH₂⁺ groups are also able to react with the phosphate. Reactions with Al-OH₂ and Al-OH₂⁺ groups by mononuclear bonding are given below.

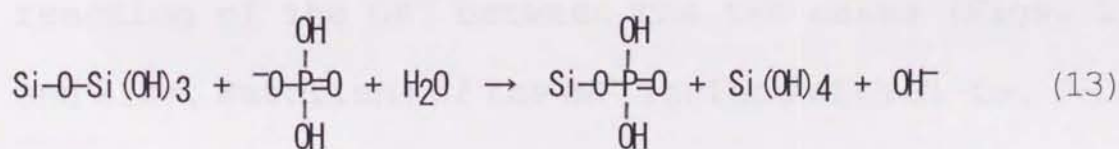




Eqs. (9) and (10) indicate no release of OH^- with the adsorption. However, if we consider further reactions for Eqs. [9] and [10], following formulae are written.



Eqs. (11) and (12) are in equilibrium, so, we can consider that initial state is the right-hand side of the equations, and the right-hand side of Eqs. (11) and (12) are just same as that of Eq. (7). Same discussions as above hold for the case of binuclear bonding. As a result, it can be assumed that one OH^- is always released initially when H_2PO_4^- reacts with any aluminol groups. When HPO_4^{2-} reacts at higher pH, two OH^- will be released. In addition to aluminol groups, part of the phosphate anion also reacts with polymeric SiO_4 tetrahedra (Fig. 1) to release Si to solution phase (Johan et al., 1997). The reaction is written as:

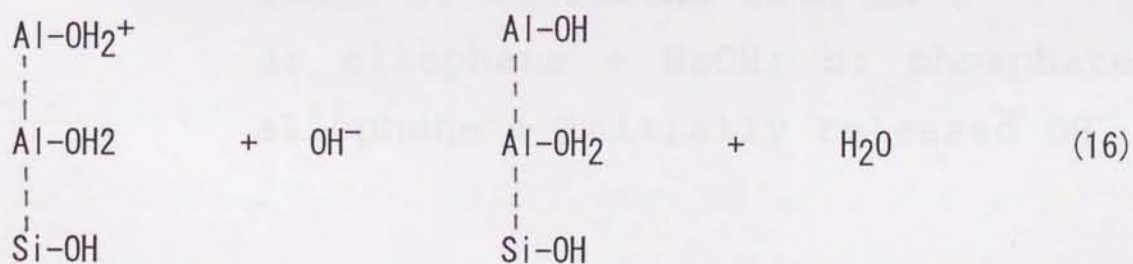
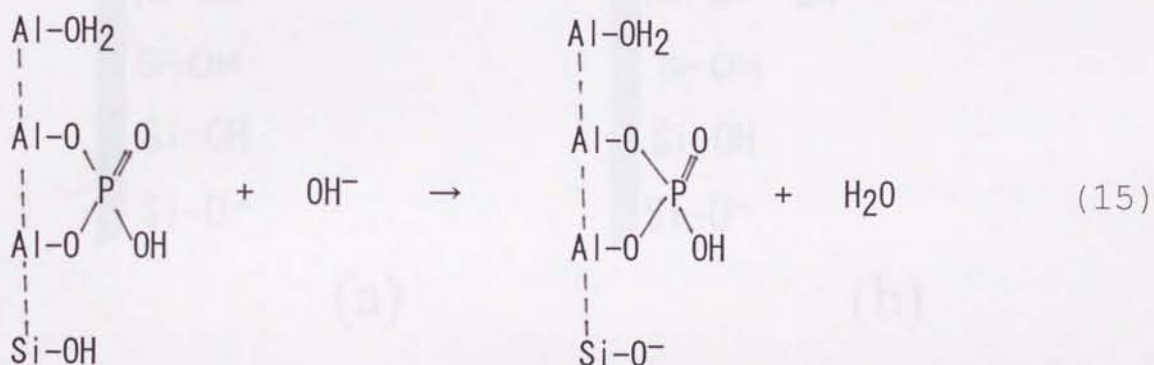
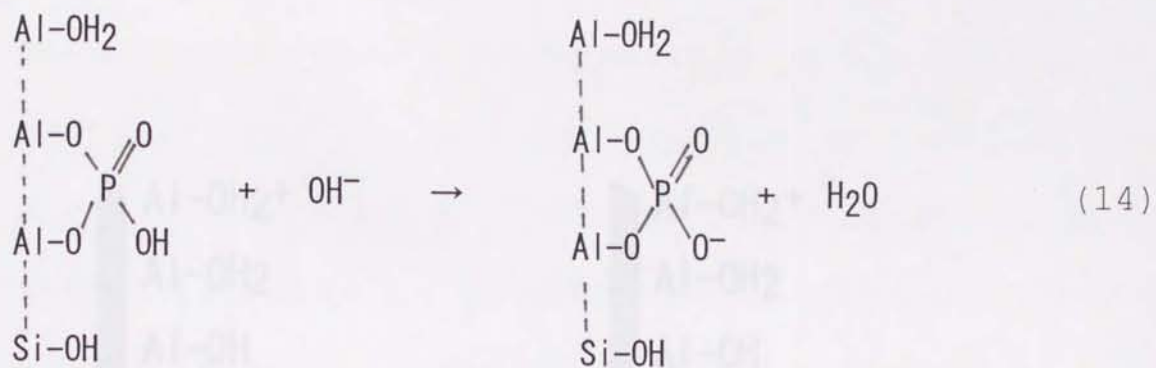


This reaction also releases one OH^- with adsorption of one H_2PO_4^- anion.

Above discussions showed that the assumption, one OH^- is initially released with adsorption of one H_2PO_4^- anion on allophane, is valid. Of course, the initially

released OH^- undergoes further reactions with allophane-phosphate adsorption complex, and the reactions will be discussed on below.

At initial stage of phosphate adsorption reaction, the adsorption complex has same amounts of negative and positive charges with the original allophane. In solution phase, OH^- ion present in same amount with the phosphate adsorbed. This situation is comparable with that when NaOH was added to original allophane in same amount with the phosphate adsorption. The two situations are schemed in Fig. 21. The difference in charge characteristics between original allophane and adsorption complex is considered as the difference in reaction of the OH^- between the two cases (Figs. 21a and 21b). Reactions of the OH^- include with Si-OH, P-OH, and Al-OH₂⁺: the former two increase negative charge and the latter decrease positive charge of the allophane and/or the complex. The reactions of initially OH^- released with the functional groups are described as follow:



Equations 14 and 15 form new negative charge, caused by de-protonation of P-OH and Si-OH, respectively.

However, according to the molecular orbital

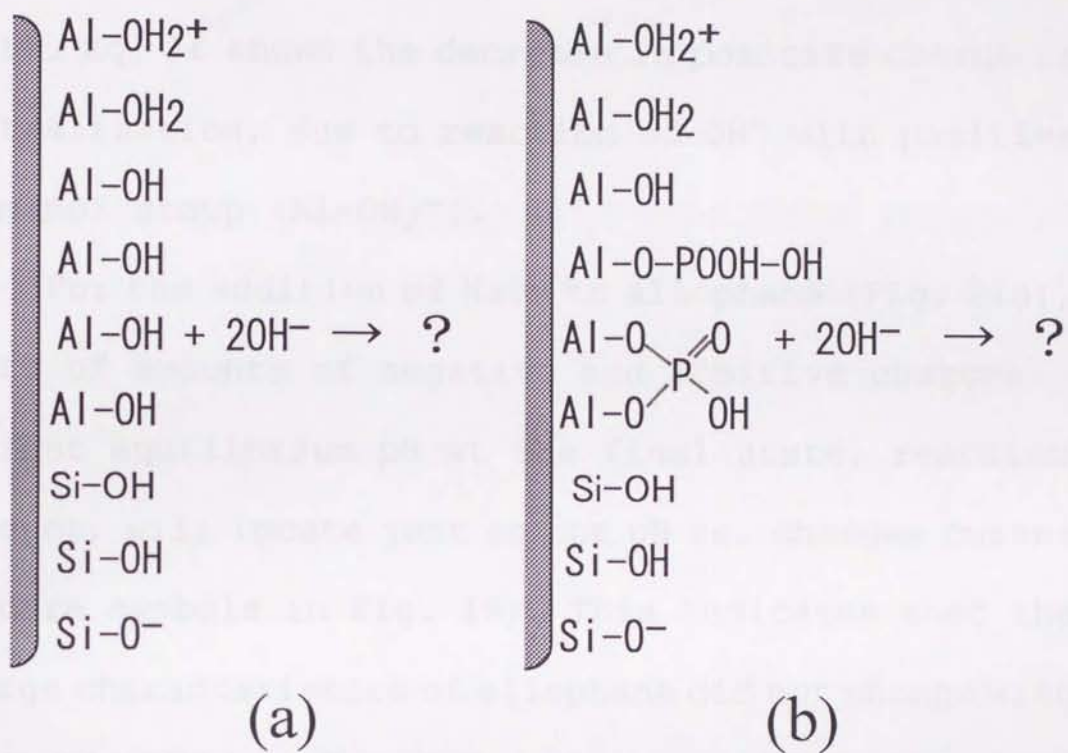


Fig. 21 Schematic representations for initial stage of reactions with OH⁻.

a: allophane + NaOH; b: phosphated allophane + initially released OH⁻

calculation result, deprotonation of Si-OH is more possible than that of P-OH (data will be shown on next part). Eq. 16 shows the decrease in positive charge or neutralization, due to reaction of OH^- with positive aluminol group (Al-OH_2^+).

For the addition of NaOH to allophane (Fig. 21a), plots of amounts of negative and positive charges against equilibrium pH at the final state, reaction product, will locate just on the pH vs. charges curves (square symbols in Fig. 19). This indicates that the charge characteristics of allophane did not change with the NaOH addition. For the complex (Fig. 21b), the plots for the reaction product located above the curve of the original allophane (circle symbols in Fig. 19). This means that more OH^- reacted with the complex to increase negative charge and decrease positive charge compared to the original allophane. Accordingly, the amount of OH^- remain in solution phase is smaller than the original allophane, resulting in lower equilibrium solution pH (Fig. 19).

One reason for the resultant more negative charge for Fig. 21b is the dissociation of P-OH group which

is not exist in Fig. 21a. Usually, the difference in amount of negative charge before and after phosphate adsorption is attributed to the presence of new acidic functional group, $P-O^-$. The resultant less positive charge for Fig. 21b is partly due to lower amount of free aluminol groups per unit mass, because some aluminol groups are blocked by the adsorbed phosphate. The decrease in the amount of free aluminol groups will also decrease the amount of positively charged aluminol groups, $Al-OH_2^+$.

In addition to the two physical effects, presence of and blocking by the adsorbed phosphate, chemical effects of the adsorbed phosphate are also possible, from analogy with organic compounds. It is well known that pKa value of a functional group of an organic compound is modified by addition or substitution reaction: for example, pKa value of phenol (9.8) is different from that of mononitro phenols (6.9-8.1). The analogy lead to the idea that the inherent functional groups of allophane, $Si-OH$ and $Al-OH_2^+$ groups, had some chemical (inductive) effects from the adsorbed phosphate. The effects may be acceleration in

dissociation reaction of Si-OH and Al-OH₂⁺ groups, resulting in more reaction with OH⁻ in solution. The chemical (inductive) effects are confirmed by theoretical molecular orbital calculations.

As described earlier, the negative charge of phosphate adsorption complex locates over the curve of CEC Vs pH of the original samples (Fig. 19), with a result the increase in pH is smaller than the original sample. Table 9 shows experimental results of pH measurement after adding NaOH with same amount of P adsorbed for each samples, 25 and 20 cmol kg⁻¹ for KyP and KnP, respectively. The mixture of allophane samples and NaOH suspension were also shaken for 24h. The results indicate that the equilibrium pHs of allophane mixed with NaOH (allophane + NaOH) are greater than that of the complexes. However at high range pH (pH>8), opposite way occurred, the equilibrium pH of the phosphate adsorption complexes was greater than that of the allophane + NaOH, for both KyP and KnP samples. This is due to at high range pH, a large part of phosphate exists as HPO₄²⁻ (two negative charges), with a result adsorption of one HPO₄²⁻ cause release of two OH⁻ at

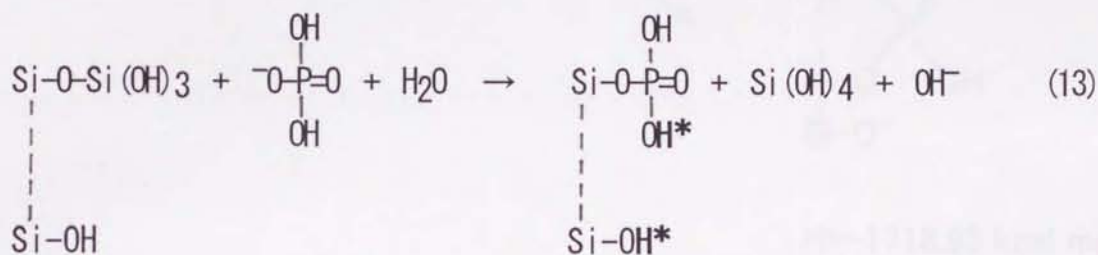
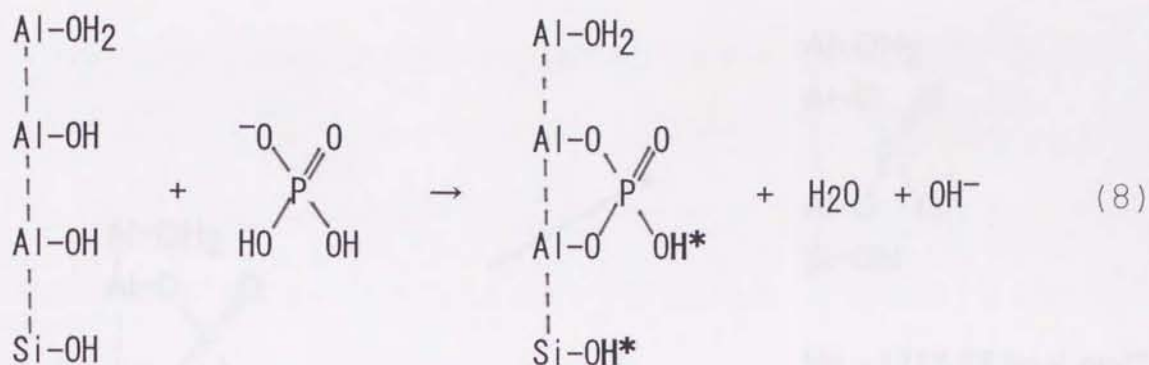
Table 9 Equilibrium solution pH after P adsorption ($K_{yP} = 25 \text{ cmol kg}^{-1}$, $K_{nP} = 20 \text{ cmol kg}^{-1}$) and after adding NaOH in same amount with P adsorbed

Initial pH	Equilibrium pH	
	After P adsorption	After adding NaOH
K_{yP}		
4.80	5.44	5.97
5.24	6.37	6.63
5.85	6.75	6.93
6.73	7.33	7.36
7.66	8.48	8.01
K_{nP}		
4.90	5.62	6.01
5.60	6.12	6.57
6.26	6.53	6.95
6.86	7.15	7.42
7.63	8.21	8.02

the initial stage. Therefore, the initial OH^- released of phosphate adsorption complex is greater than that of allophane + NaOH. Hence, remain OH^- in the solution phase (increase in pH) is greater for the P adsorption complex than that for the allophane + NaOH.

5-3-3 Molecular Orbital Analysis

As mentioned above, OH^- was initially released just the same amount with the P adsorbed, on the first stage of phosphate reaction on allophane. Molecular orbital calculation was done to confirm whether the initially released OH^- released react with P-OH or Si-OH groups. The calculation was carried out with method as described previously. The analysis was done for two P adsorption products: phosphate (H_2PO_4^-) adsorbed on the two aluminol groups (binuclear complex) and on weakly bonded SiO_4 tetrahedra (replacement reaction). The two reaction products were previously presented as Eqs. (8) and (13), and are shown again below:



Protons with star marks represent the protons which will dissociate and react with OH^- to form H_2O .

Calculation results are shown in Fig. 22. Small molecules such as OH^- and H_2O were neglected for simplicity. So we can compare H (heat of formation) values of the products only. Lower in the H value indicates that more possible in the reaction.

Calculation results indicated that dissociation of proton from silanol group (Si-OH) resulted in lower H value than that from P-OH group, for both reactions.

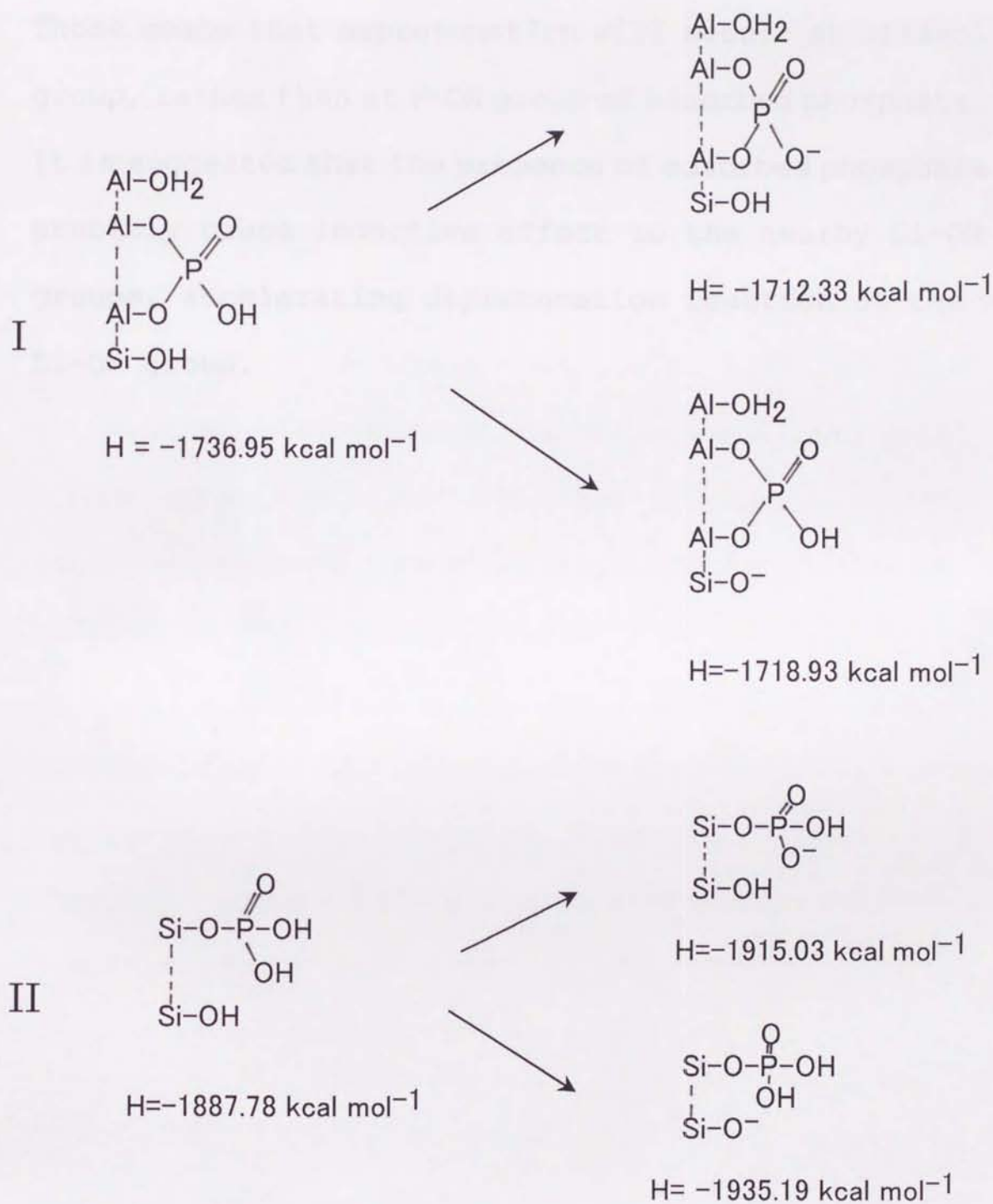


Fig. 22 Calculated H (heat of formation) of some molecules. I: phosphate bonded on two aluminol groups, II: phosphate replaced SiO₄ tetrahedra

Those means that deprotonation will occur at silanol group, rather than at P-OH group of adsorbed phosphate. It is suggested that the presence of adsorbed phosphate probably cause inductive effect to the nearby Si-OH groups, accelerating deprotonation reaction of the Si-OH group.

5-4 Conclusions

Net change in surface negative and positive charges of allophane and other clay minerals, with adsorption of phosphate and other adsorbates, have not been estimated exactly. The net change is calculated as observed change minus that due to solution pH increase with the adsorption. To explain reasons for the net change in surface charges, the study compared reactions with OH^- between original and phosphated allophanes under assumption that one OH^- is initially release to solution with one anion adsorption. This way of thinking is simple in discussing on modification of surface charge characteristics of allophane with phosphate adsorption, and also applicable for other combinations of adsorbent and adsorbate.

Chapter 6 IMPLICATIONS OF THIS STUDY FOR AGRICULTURE AND ENVIRONMENT

Until now, phosphate fixation in soils becomes problem for agriculture, due to applied phosphorus fertilizer are not available for plant growth. However, the study found that the P adsorption on allophane give positive effect to the allophane, such as decrease in AEC, and increase in CEC. The increase in CEC has meaning the enhancement in capacity to retain nutrients for plants. The results of the study can be applied for Andepts, which contains allophane as main clay components.

Furthermore, the study also found that the P adsorption increase pH solution. Other previous studies also found the same results for soils or other clay minerals. This phenomenon also has positive effect for the soil fertility, especially for acid soils.

In view of environment, allophane, as a phosphorus adsorbent can be applied as a material to prevent eutrofication in water reservoirs. In the present study, natural allophane was used, but in the future

artificial allophane may be produced, not only in laboratory scale, but also in industrial scale, such as artificial zeolite. To prevent the eutrofication, allophane with low Si/Al ratio is better than that with high ratio, due to it has higher capacity for P adsorption.

The finding of increase in surface acidity can be also developed in catalyze science. Allophane-phosphate adsorption complex may catalyze some polymerization reaction such as other clay minerals. As catalysis allophane with high Si/Al ratio is better than that with low Si/Al ratio, due to its stronger acidity .

REFERENCES

- Benesi, H.A., (1956) Acidity catalyst surfaces. I. Acid strength form colors of adsorbed indicators. *J. Am. Chem. Soc.*, **78**, 5490-5494.
- Cooke, G.W. and Williams, R.J.B. (1973) Significance of man-made sources of phosphorus: fertilizer and farming. The phosphorus involved in agricultural system and possibilities of its movement into natural water. In: Jenkins, S.H. and Ives, K.J. (Eds.) Phosphorus in fresh water and the marine environment. Pergamon Press, Oxford. 111-128.
- Davenport, W.H., (1949) Determination of aluminum in presence of iron. *Anal. Chem.*, **9**, 873-878.
- Enfield, C.G. and Ellis, JR.R. (1986) The movement of phosphorus in soil. In: D.M. Kral (Ed.) Chemical mobility and reactivity in soil systems. *Soil Sci. Soc. Am.*, American Soc. Agron. Madison, Wisconsin. 93-107.
- Farmer, V.C., Fraser, A.R., Russel, J.D. and Yoshinaga, N. (1977) Recognition of imogolite structures in allophanic clays by infrared spectroscopy. *Clay Miner.* **12**, 55-57.

- Farmer, V.C., Russel, J.D. and Berrow, M.L. (1980) Imogolite and proto-imogolite allophane in spodic horizon: evidence for a mobile aluminum silicate complex in podzol formation. *J. Soil Sci.*, **31**, 673-684.
- Frenkel, M. (1974) Surface acidity of montmorillonites. *Clays and Clay Minerals*. **22**, 435-441.
- Goldberg, S. and Sposito, G. (1985) On the mechanism of specific phosphate adsorption by hydroxylated mineral surfaces: a review. *Communications in Soil Science and Plant Analysis*. **16**, 801-821.
- Gunjigake, N. and Wada, K. (1981) Effect of phosphorus concentration and pH on phosphate retention by active aluminum and iron of Ando soils. *Soil Sci.*, **132**, 347-352.
- Harada, Y. and Wada, K. (1973) Release and uptake of protons by allophanic soils in relation to their CEC and AEC. *Soil Sci. Plant Nutr.*, **19**, 73-82.
- Hawthorne, D.G. and Solomon, D.H. (1972) Catalytic activity of sodium kaolinites. *Clays and Clay Minerals*, **20**, 75-78.
- Henmi, T. (1977) The dependence of surface acidity on chemical composition ($\text{SiO}_2/\text{Al}_2\text{O}_3$ molar ratio) of

- allophane. *Clay Miner.*, **12**, 356-358.
- Henmi, T. (1980) Effect of $\text{SiO}_2/\text{Al}_2\text{O}_3$ ratio on thermal reactions of allophane. *Clays Clay Miner.*, **28**, 92-96.
- Henmi, T. (1985) Importance of chemical composition ($\text{SiO}_2/\text{Al}_2\text{O}_3$ ratio) as factor affecting physicochemical properties of allophanes from weathered volcanic ash and pumice. In: J. Konta (Ed.) 5th Meeting of European Clay groups, 459-464.
- Henmi, T., Matsue, N. and Johan, E. (1997) Change in the surface acidity of allophane with a low Si/Al ratio by reaction with ortho-silicic acid. *Jpn. J. Soil Sci. Plant Nutr.*, **68**, 514-520 (in Japanese with English abstract).
- Henmi, T., Matsue, N. and Son, L.T. (1998) Change in surface properties of allophane and imogolite by fluoride ion treatment -Increase in surface acid strength and cation exchange capacity following treatment and their molecular orbital analysis-. *Jpn. J. Soil Sci. Plant Nutr.*, **69**, 470-476 (in Japanese with English abstract).
- Henmi, T., Tange, K., Minagawa, T. and Yoshinaga, N.

- (1981) Effect of $\text{SiO}_2/\text{Al}_2\text{O}_3$ ratio on the thermal reactions of allophane. II. Infrared and X-ray powder diffraction data. *Clays Clay Miner.*, **29**, 124-128.
- Henmi, T. and Wada, K. (1974) Surface acidity of imogolite and allophane. *Clay Minerals*. **10**, 231-244.
- Henmi, T. and Wada, K. (1976) Morphology and composition of allophane. *Am. Miner.*, **61**, 379-390.
- Higashi, T. and Ikeda, H. (1974) Dissolution of allophane by acid oxalate solution. *Clay Sci.*, **4**, 205-221.
- Hook, J.E. (1986) Movement of phosphorus and nitrogen in soils following application of municipal waste water. In: Kral, D.M. (Ed.) *Chemical mobility and reactivity in soil systems*. Soil Sci. Soc. Am. American Soc. Agron. Madison, Wisconsin. 241-255.
- Huang, W. D. and Johns, W. D. (1966) Simultaneous determination of fluorine and chlorine in silicate rocks by rapid spectrophotometric method. *Anal. Chim. Acta*, **37**, 508-515.
- Johan, E., Matsue, N., and Henmi, T. (1997) Phosphate adsorption on nano-ball allophane and its molecular orbital analysis. *Clay Sci.*, **10**, 259-270.

- Matar, A., Torrent, J. and Ryan, J. (1992) Soil and fertilizer phosphorus and crop response in the dryland Mediterranean zone. *Adv. Soil Sci.*, **18**, 82-146.
- Matsue, N. and Henmi, T. (1993) Molecular orbital study on the relationship between Si/Al ratio and surface acid strength of allophane. *J. Clay Sci. Soc. Jpn.*, **33**, 102-106 (in Japanese with English abstract).
- Mehra, O.P. and Jackson, M.L. (1960) Iron oxide removal from soils and clays by a dithionite-citrate system buffered with sodium bicarbonate. In: Earl Ingerson (Ed.) *Seventh National Conference of Clays and Clay Minerals. Monograph No. 5*. Pergamon Press. London. 317-327.
- Mekaru, T. and Uehara, G. (1972) Anion adsorption in ferruginous tropical soils. *Soil Sci. Soc. Am. Proc.*, **36**, 296-300.
- Mitchel, B.D., Farmer, V.C. and McHardy, W.J. (1964) Amorphous inorganic materials in soils. *Adv. Agron.*, **16**, 327-383.
- Mortland, M.M. and Raman, K.V. (1968) Surface acidity of smectites in relation to hydration, exchangeable cation, and structure. *Clays and Clay Minerals*. **16**,

393-398.

Murphy, J. and Riley, J. P. (1962) A modified single solution method for determination of phosphate in natural waters. *Anal. Chim. Acta*, **27**, 31-36.

Naidu, R., Syer, J. K., Tillman, R. W. and Kirkman, J. H. (1990) Effect of liming and added phosphate on charge characteristics of acid soils. *J. Soil Sci.*, **41**, 156-164.

Nanzyo, M. (1988) Phosphate adsorption on the clay fraction of Kanuma Pumice. *Clay Sci.*, **7**, 89-96.

Nanzyo, M. (1995) Reactions of phosphate with soil colloids. *J. Clay Sci. Soc. Jpn*, **35**, 108-119 (in Japanese with English abstract).

Nanzyo, N. and Watanabe, Y. (1982) Diffuse reflectance infrared spectra and ion-adsorption properties of the phosphate surface complex on goethite. *Soil Sci. Plant Nutr.*, **28**, 359-369.

Parfitt, R.L. (1978) Anion adsorption by soils and soils materials. *Adv. Agron.*, **30**, 1-50.

Parfitt, R. L. (1980) Chemical properties of variable charge soils. In *Soils with Variable Charge*, Ed. Theng, B. K. G., p. 167-194, New Zealand Soc. Soil Sci., Soil Bureau, DSIR, Lower Hutt, New Zealand.

- Parfitt, R.L., Furkert, R.J., and Henmi, T (1980)
Identification and structure of two types of
allophane from volcanic ash soils and tephra. *Clay
Clay Miner.*, **28**, 328-334.
- Parfitt, R. L. and Henmi, T. (1980) Structure of some
allophanes from New Zealand. *Clays Clay Miner.*, **28**,
285-294.
- Paterson, E. (1977) Specific surface area and pore
structure of allophanic soil clays. *Clay Miner.*, **12**,
1-9.
- Rajan, S.S.S. (1975) Phosphate adsorption and the
displacement of structural silicon in an allophane
clay. *J. Soil Sci.*, **26**, 250-256.
- Rajan, S. S. S. (1976) Change in net surface charge of
hydrous alumina with phosphate adsorption. *Nature*,
262, 45-46.
- Sawhney, B. L. (1974) Charge characteristics of soils
as affected by phosphate sorption. *Soil Sci. Soc.
Am. Proc.*, **38**, 159-160.
- Schalscha, E. B., Pratt, P. F., and Soto, D. (1974)
Effect of phosphate adsorption on the cation-
exchange capacity of volcanic ash soils. *Soil Sci.
Soc. Am. Proc.*, **38**, 539-540.

- Shimizu, H., Watanabe, T., Henmi, T., Masuda, A. and Saito, A. (1988) Study on allophane and imogolite by high-resolution solid-state ^{29}Si - and ^{27}Al -NMR and ESR. *Geochem. J.*, **22**, 23-31.
- Siggel, M.R. and Thomas, T.D. (1986) Why are organic acids stronger acids than organic alcohols? *J. Am. Chem. Soc.* **108**, 4360-4363.
- Siggel, M.R., Thomas, T.D. and Saethre, L.J. (1987) AB initio calculation of Brønsted acidities. *J. Am. Chem. Soc.*, **110**, 91-96.
- Solomon, D.H. (1968) Clay minerals as electron acceptors and/or electron donors in organic reactions. *Clays and Clay Minerals*, **16**, 31-39.
- Solomon, D.F. and Murray, H.H. (1972) Acid-base interactions and the properties of kaolinite in non-aqueous media. *Clays and Clay Minerals*. **20**, 135-141.
- Son, L. T., Matsue, N. and Henmi, T. (1998) Boron adsorption on allophane with nano-ball morphology. *Clay Sci.*, **10**, 315-325.
- Stewart, J.J.P. (1989a) MOPAC ver.6. QCPE#455.
- Stewart, J.J.P. (1989b) Optimization of parameters for semi-empirical methods. I. Method. *J. Comput. Chem.*,

10, 209-220.

Strickland, J.D.H. and Parsons, T.R. (1968) A practical handbook of sea water analysis. Bull. Fish. Res. Bd. Canada, No. 167.

Syers, J.K., Browman, M.G., Smillie, G.W. and Corey, R.B. (1973) Phosphate sorption by soils evaluated by the Langmuir adsorption equation. Soil Sci. Am. Proc., **37**, 358-363.

Tanabe, K. (1970) Solid acids and bases, their catalytic properties. Kodansha, Tokyo.

Tsuzuki, Y. and Nagasawa, K (1960) A study of exothermic reaction of allophane (in Japanese). Adv. Clay Sci. (Tokyo) **2**, 377-384.

Van Olphen, H. (1971) Amorphous clay materials. Science, **171**, 90-91.

Wada, K. (1989) Allophane and imogolite. In Minerals in Soil Environments (2nd ed.), Eds. Dixon, J. B. and Weed, S. B., p. 1051-1088, Soil Sci. Soc. Am., Madison.

Wada, S. (1983) pH- and ionic concentration-dependence of monovalent cation retention by clays and clay minerals expected in soils. Soil Sci. Plant Nutr.,

29, 561-564.

Wada, S. and Wada, K. (1977) Density and structure of allophane. *Clay Miner.*, **12**, 289-298.

Walling, C. (1950) The acid strength of surfaces. *J. Am. Chem. Soc.*, **72**, 1164-1168.

Woodruff, J.R. and Kamprath, E.J. (1965) Phosphorus adsorption maximum as measured by the Langmuir isotherm and its relationship to phosphorus availability. *Soil Sci. Soc. Am. Proc.* **29**, 148-150.

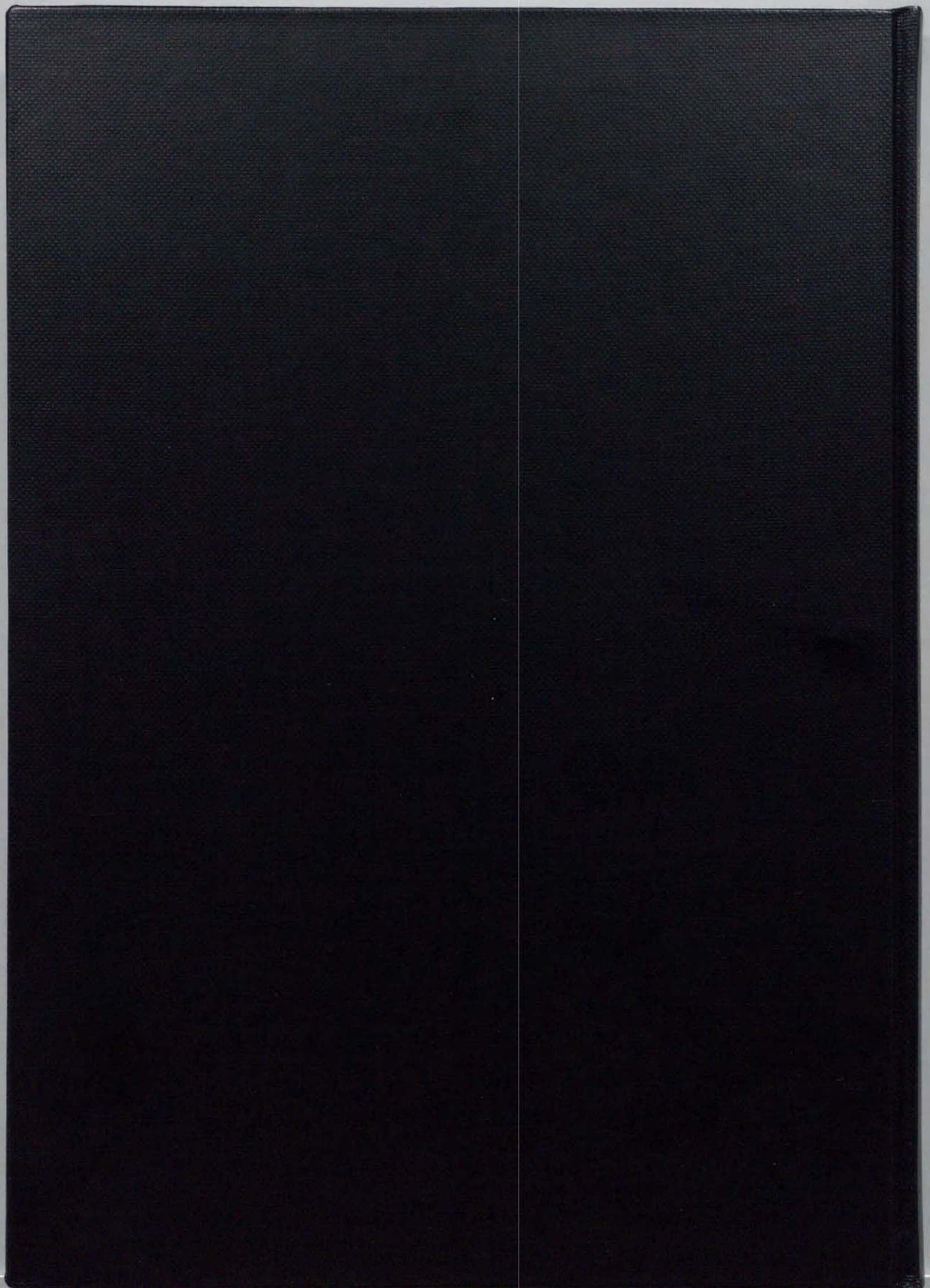
Wu, D.Y., Matsue, N., Henmi, T. and Yoshinaga, N. (1992) Surface acidity of pyrophyllite and talc. *Clay Sci.*, **8**, 367-379.

Yoshinaga, N. and S. Aomine (1962) Allophane in some Ando soils. *Soil Sci. Plant. Nutr.* **8**, 22-29.

APPENDIX 1

Equilibrium pH of the allophane samples after the P adsorption

Initial P concentration	Equilibrium pH	
	KyP	KnP
Na Background solution		
0	5.67	5.99
200	6.36	6.32
400	6.08	6.25
600	6.01	6.18
800	5.98	6.14
1000	5.91	6.08
1200	5.92	6.01
1400	5.81	6.01
1600	5.84	5.96
1800	5.68	5.95
1000	5.74	5.90
Ca Background solution		
0	5.11	6.17
200	5.35	5.95
400	5.39	5.90
600	5.41	5.82
800	5.36	5.78
1000	5.37	5.78
1200	5.26	5.69
1400	5.24	5.63
1600	5.22	5.62
1800	5.21	5.59
2000	5.18	5.57



inches 1 2 3 4 5 6 7 8
cm 1 2 3 4 5 6 7 8 9 10 11 12 13 14 15 16 17 18 19

Kodak Color Control Patches

© Kodak, 2007 TM: Kodak

Blue	Cyan	Green	Yellow	Red	Magenta	White	3/Color	Black
1	2	3	4	5	6	7	8	9
10	11	12	13	14	15	16	17	18
19	20	21	22	23	24	25	26	27

Kodak Gray Scale



© Kodak, 2007 TM: Kodak

A 1 2 3 4 5 6 M 8 9 10 11 12 13 14 15 B 17 18 19

